Magnetic and Thermal Properties of Dysprosium Aluminum Garnet. II. Characteristic Parameters of an Ising Antiferromagnet*

W. P. Wolf, B. Schneider,† D. P. Landau,‡ and B. E. Keen§
Becton Center, Yale University, New Haven, Connecticut 06520
(Received 1 November 1971)

Extensive earlier work has indicated that dysprosium aluminum garnet (DAG) in a magnetic field along a ⟨111⟩ axis should approximate to a two-sublattice Ising-model antiferromagnet, and in this paper we examine this correspondence critically. Quantitative estimates are derived for the differences between the ideal model and the real material, and it is shown that they are in fact very small and that appropriate corrections can be applied to allow for most of the deviations. General expressions based on the Ising model are derived for the magnetization, differential susceptibility, and specific heat in field and temperature regions where exact asymptotic expansions are valid, and these are fitted to available experimental data on DAG. The results of the analysis can be expressed in terms of two sets of parameters which describe, respectively, the single-ion properties and combinations of the spin-spin interactions. The relation of these parameters to the microscopic Hamiltonian is deferred to a later paper, but a number of empirical cross checks indicate excellent consistency in the results. In addition, a number of parameters describing the cooperative behavior are extracted from the experimental data and there is a discussion of some of the general problems of analyzing critical-point data. The significance of most of these parameters must await further theoretical work on Ising models with competing and long-range interactions.

I. INTRODUCTION

In a previous paper,[1] which we shall henceforth refer to as I, we described a series of magnetic and thermal measurements on single crystals of dysprosium aluminum garnet (DAG) with magnetic fields applied along one of the ⟨111⟩ directions. The results, together with those of numerous earlier experiments referred to in I, showed that DAG undergoes an unusual and interesting magnetic phase transition at low temperatures, which is dominated by an extremely high magnetic anisotropy. As a result of this, there is no spin-flop phase as commonly found in antiferromagnets,[2] and the properties resemble those of a simple two-sublattice Ising model in a magnetic field. It is the purpose of the present paper to pursue this correspondence in some detail and to extract from the data a number of parameters characteristic of the Ising model.

In particular, we shall show that one can define a number of characteristic parameters which do not require explicit knowledge of the microscopic details of the corresponding Ising model, but which can still be used to describe the system accurately for fields and temperatures far from the phase transition. The parameters are of two kinds: "single-ion" parameters which do not depend on the spin-spin interactions, such as g values, Curie constants, and the Van Vleck temperature-independent susceptibility, and "collective parameters" which include the Curie-Weiss constant and the energy gap for elementary excitations at $T = 0\,^{\circ}\mathrm{K}$.

Given a specific Ising-model Hamiltonian such parameters can of course be related to the microscopic interactions, and indeed such an analysis can be used to determine the terms in the Hamiltonian and to check the validity of the Ising-model approximation. However, we choose to defer this part of the analysis until we can include the results of additional experiments with magnetic fields applied in directions other than ⟨111⟩ and these we plan to discuss in a separate paper in the present series.[3] The detailed microscopic analysis will therefore not be given until Paper IV.[4]

For the present we shall therefore restrict ourselves to an analysis of the temperature and field variations of observable properties with H along ⟨111⟩, in those regions where asymptotically exact expressions can be obtained in terms of appropriate combinations of microscopic interactions. The advantage of such an approach is that it emphasizes the essential simplicity of DAG without introducing the geometrical complexity of the garnet structure, which only becomes important in the final microscopic analysis.

In order to establish the correspondence with a simple Ising model it is necessary to show that at least three conditions are satisfied: (i) Each Dy^{3+} ion can be represented completely by an effective spin $S' = \frac{1}{2}$. (ii) The effective interaction between neighboring spins is given by terms of the form $S'_{zi} S'_{zj}$. (iii) The interaction of each spin with an applied magnetic field is given by $g_{ei} \mu_B S'_{zi} H_z$, where the effective g factors g_{ei} are preferably equal for all i.

We shall consider these conditions in connection with the complete Hamiltonian for DAG in Sec. II, and we shall show that we would indeed expect the

correspondence to be very close, at least for the case of H along $\langle 111 \rangle$. For other orientations of H the correspondence is more complex, and we shall defer the discussion of this to Paper III.

Taking the Ising model as a working approximation we shall derive in Sec. III expressions for the magnetization and specific heat for "high" and "low" fields and temperatures, where "high" and "low" are suitably defined in terms of appropriate relative energies. The derived expressions should be applicable generally to all Ising-like systems, and in Sec. IV we use them specifically to extract the appropriate parameters for DAG from the data presented in I.

In addition to parameters which can be related to theories which are asymptotically exact far from the phase transition, one can also extract from the data "critical parameters" which characterize the phase transition and a number of these will be obtained in Sec. IV B. Such parameters include the Néel temperature and its variation with field, the temperature for the onset of the first-order transition (the tricritical point),[1,5] and the parameters describing the singularity in the specific heat. The comparison of these parameters with theory would entail very much more complicated statistical approximations than the expansions involving the "collective parameters" far from the phase transition, and at this stage we present them essentially as empirical results.

All three sets of parameters, the single ion, collective, and critical, are summarized in five tables (Tables II–VI) which include both results obtained from the present work as well as from previous studies.

II. HAMILTONIAN

A. Effective-Spin Approximation

The low-lying energy levels of the Dy^{3+} ion have been studied extensively by microwave resonance[6] and optical spectroscopy.[7–14] It was found that all ions are magnetically equivalent except for their orientation with respect to the crystal axes, as expected from the known crystal structure,[15–17] and that the energy separation between the lowest Kramers doublet and the first excited state, E_1, is about 70 cm^{-1} ($\sim 100\,^\circ K$). At temperatures in the liquid-helium range, therefore, the population of the first excited state is entirely negligible, and providing that the effects of magnetic fields and other interactions are also small compared with E_1, each ion can be accurately described in terms of the two states spanning this doublet. Within this manifold any operator can then be represented completely by an equivalent operator expressed in terms of the components of an effective spin $S' = \frac{1}{2}$.

In particular the linear Zeeman effect can be represented by $\mu_B \vec{H} \cdot \overleftrightarrow{g} \cdot \vec{S}'$, where $\overleftrightarrow{g}$ defines the magnetic properties of the doublet. For garnets the principal axes of $\overleftrightarrow{g}$ coincide with the local D_2 axes at each site, and the orientation of these axes has been discussed in a number of earlier publications.[18] For the present we want to consider only the case of fields applied along one of the $\langle 111 \rangle$ *crystal* axes, and for this orientation half the ions will have an effective g factor given by[19] $g_{e1} = (\frac{1}{3} g_z^2 + \frac{2}{3} g_x^2)^{1/2}$ while for the other half $g_{e2} = (\frac{1}{3} g_z^2 + \frac{2}{3} g_y^2)^{1/2}$, where g_x, g_y, and g_z are the three principal values of $\overleftrightarrow{g}$. There is a considerable amount of evidence[6,8,10,11,20–22] that $g_z \gg g_x$, g_y with $g_z \approx 18$, but the accurate determination of g_x and g_y presents a major difficulty since they appear to be extremely small and errors can easily arise from small misalignments. The best quantitative estimate at present is based on optical measurements[11] and this gives $g_x \approx g_y \approx 0.5 \pm 0.2$. However recent Mössbauer experiments[23] indicate that the values may be even smaller, with $|g_x \pm g_y| < 0.5$.[24] In any case, it seems a very good approximation to neglect both g_x^2 and g_y^2 in the expressions for g_{e1} and g_{e2} and to take

$$g_e = (1/\sqrt{3}) g_z \tag{1}$$

for all sites, when $\vec{H}$ is parallel to $\langle 111 \rangle$.

We have discussed this particular point at some length because we want to emphasize the fact that the spins are not quite identical magnetically, and that g_{e1} and g_{e2} might in fact differ by as much as 0.1% for the two types of sites. For most purposes such a difference would be entirely negligible, but it could become relevant in the analysis of the high-resolution data of the field-induced first-order phase transition. However, in general we can certainly use Eq. (1), which is physically equivalent to considering only components of $\vec{H}$ along the local z axis of each spin.

B. Ising-Model Approximation

From the observed g-value anisotropy one can make some general statements about the nature of the ground-state doublet and a qualitative prediction that the interactions coupling different neighbors might be Ising-like.[25] However, in order to make a more quantitative statement about the validity of the Ising-model approximation one requires considerably more information and a detailed analysis is, in fact, quite difficult.

From the large value of g_z we can infer that the ground state must be predominately $|J = \frac{15}{2}, J_z = \pm \frac{15}{2}\rangle$ but the details of the admixtures allowed by D_2 symmetry ($\Delta J_z = 2, 4, 6\ldots$) can only be obtained from a full crystal-field analysis. Two such analyses have recently been reported, one by Grünberg *et al.*[12] using optical data for Dy^{3+} diluted into yttrium aluminum garnet (YAG) and the other by Wadsack *et al.*[14] using Raman-scattering data for

pure DAG. The two analyses are in general agreement and the one for pure DAG has been used[26] to calculate a detailed description of the ground-state doublet. Nonzero admixtures of altogether 52 basis states were found, but most of these were very small. The dominant terms were

$$0.824\left|\pm\tfrac{15}{2}\right\rangle+0.520\left|\pm\tfrac{11}{2}\right\rangle+0.141\left|\pm\tfrac{7}{2}\right\rangle-0.159\left|\pm\tfrac{3}{2}\right\rangle$$
$$-0.008\left|\mp\tfrac{1}{2}\right\rangle+0.027\left|\mp\tfrac{5}{2}\right\rangle+0.044\left|\mp\tfrac{9}{2}\right\rangle+0.019\left|\mp\tfrac{13}{2}\right\rangle, \quad (2)$$

where each of these components belongs to the $^6H_{15/2}$ term and we specify J_z along the local g_z axis. Admixtures of all other states were less than 0.03.

The coupling of two ions specified by such states can obviously be quite complex and in general we might expect an effective spin-spin interaction of the most general form $\vec{S}'_i \cdot \overleftrightarrow{\mathcal{J}}_{ij} \cdot \vec{S}'_j$. However, we note that the off-diagonal matrix elements of all operators which transform like vectors (which are nonzero for $\Delta J_z = \pm 1$) will be relatively small, consistent with the anisotropy of the Zeeman effect, and any interactions involving only products of vector operators will therefore be mainly diagonal. This includes magnetic dipole-dipole coupling and the isotropic part of the exchange interaction, and to the extent that these are dominant we might therefore expect a predominately Ising-like coupling.

However, it is always possible that there might be sizable interactions of a more complex form, such as quadrupole-quadrupole or anisotropic exchange, and indeed evidence for such terms has been found in other rare-earth insulators.[27,28] Such interactions would generally not be diagonal within the states given by Eq. (2), and in terms of the spin Hamiltonian this would imply non-Ising forms such as $\mathcal{J}_{xx} S'_{xi} S'_{xj}$.

In the absence of a detailed microscopic theory for the actual interactions in DAG we must resort to additional experimental data to place an upper limit on such terms. Fortunately such a limit can be obtained readily from the observed fact that the Mössbauer spectrum at 4.2 °K shows the fully resolved hyperfine structure[23] even though ordering does not start until 2.5 °K. This implies an unusually slow electron spin-spin relaxation time $\tau_{ss} \gtrsim 10^{-8}$ sec, and using a simple uncertainty-principle argument this puts an upper limit of 10^{-3} °K on the largest of the non-Ising $\mathcal{J}$'s. In fact this limit represents the sum of the different nonsecular interactions between all neighbors as well as the effects of other possible relaxation mechanisms, and we might therefore conjecture that the individual $\mathcal{J}$'s might be at least an order of magnitude smaller. This can be compared to the Ising-like terms which are typically 0.1–0.7 °K,[25] so that we can conclude that the Ising model should indeed be quite a good approximation for the interactions in DAG.

As in the case of the g_e, we must caution that this approximation might well break down in some critical regions, and it will certainly be important for all relaxation effects. However, for most properties we can write an effective interaction Hamiltonian of the form

$$\mathcal{H} = \sum_{i>j} K_{ij}\sigma_i\sigma_j + \tfrac{1}{2} g_e \mu_B H \sum_i \sigma_i \,, \quad (3)$$

where we have changed from $S'_{zi} = \pm\frac{1}{2}$ to $\sigma_i = \pm 1$ to conform to the usual Ising-model notation, and we have also included the term corresponding to an applied field along $\langle 111 \rangle$.[29]

The coupling constants K_{ij} will generally not be restricted to any particular near neighbors, since we know that magnetic dipole-dipole coupling will play some role in DAG, as it does in all real crystals. Since DAG is a relatively dense material with a large magnetic moment per spin, we might expect the cumulative effects of the long-range interactions to be larger than usual, and indeed we have already shown in I that this leads to a marked shape dependence of the magnetic and thermal properties. For the purposes of the present paper, this shape dependence will be important only insofar as the fitted parameters must be determined for specified shapes, but in the final microscopic analysis the long-range dipole sums will have to be evaluated explicitly.

Moreover, it will be important to note that the magnitudes and signs of the K's for different near neighbors could well be such as to produce a competition between different magnetic states, and in this respect DAG will be more complex than the usual nearest-neighbor Ising model. However, away from the phase-transition region these complications will not affect the form of the asymptotic expressions and we can use simple Ising-model ideas.

C. Minor Complications and Corrections

In addition to the intrinsic approximations implicit in Eq. (3), there are a number of relatively minor complications which must be considered before a comparison with the experimental results is possible. The effects are all very small and it is convenient to remove them by applying appropriate corrections to the data before analyzing the more interesting cooperative properties.

1. Excited Electronic States

As explained above, the first excited electronic state lies at an energy of about 100 °K and its population at 4.2 °K is thus negligible. However, some of the specific-heat measurements extended up to 8 °K, and for these one must allow for a small contribution from the excited state. The contribution

is readily estimated as

$$C_{\text{Schottky}}/R = (E_1/k_BT)^2 \exp(-E_1/k_BT) ,$$

and this amount was subtracted from all measurements. The largest correction was about 2%. There is also a small contribution to the susceptibility due to the population of the first excited state, but even at the highest temperatures of our measurements (20 °K) the effect was less than 0.3% and could be neglected.

2. *Van Vleck Paramagnetism and Diamagnetism*

In addition to the linear Zeeman effect there is a term quadratic in the field, and even for small H this contributes a finite term to the magnetic susceptibility. The major part of this arises from admixtures of excited electronic states[30] and there is also a small negative contribution due to diamagnetism. Both effects are independent of all the other magnetic effects, and they simply contribute an additional moment

$$m = \chi_{VV} H_1 - \chi_{\text{dia}} H_2 , \tag{4}$$

where H_1 and H_2 are appropriate local magnetic fields. The accurate computation of H_1 and H_2 in a complex system such as DAG is actually quite difficult since one must note that χ_{VV} will be anisotropic for each type of site. Thus the individual contributions to m will generally not be parallel to the applied field, or to the total magnetic moment M, even though both χ_{VV} and χ_{dia} for the whole crystal must be isotropic by cubic symmetry. Fortunately the effects on DAG are very small and we can readily derive an approximate expression for m which is sufficiently accurate. The diamagnetic contribution can be estimated from earlier measurements[31] on $Yb_3Ga_5O_{12}$, which show that $\chi_{\text{dia}} \sim -2\times10^{-6}$ emu/cm^3 which as we shall find is negligible compared with χ_{VV}. For the Van Vleck term we need an expression for H_1 and this can be estimated using mean field theory and assuming only magnetic dipole interactions. The result is[32]

$$m \approx \chi_{VV}(H_0 + aM) , \tag{5}$$

where $a = 1.5$ Oe cm^3/emu and χ_{VV} is found from the experimental data to be $(12.3 \pm 1.0)\times10^{-4}$ emu/cm^3 (see Sec. III D). A correction of this magnitude was subtracted from all the data and in general this involves a negligible error. Thus at 10 kOe and 1.1 °K the contribution of m is less than 2% and the uncertainty is less than a tenth of this.

However, there are two regions where the effect of χ_{VV} becomes very important, and neglecting it would cause a serious error in the analysis of the data. The two regions are the low- and high-temperature ends of the low-field susceptibility measurements, where the electronic susceptibility becomes small and therefore comparable with the temperature-*independent* χ_{VV}. Fortunately, M is small under these conditions, and the approximate calculation of the constant a in Eq. (5) introduces no significant error. However, it is necessary to estimate χ_{VV} as accurately as possible, and this can best be done by finding the slope of the high-field low-temperature magnetization curve (see Sec. III D.)

3. *Phonon Effects*

The principal effect of the crystal lattice is the contribution of a phonon specific heat which must be subtracted from the measured data to extract the electronic properties. Since DAG orders at a relatively low temperature this contribution is extremely small in the critical region, and the only sizable correction which must be applied is at the highest measured temperatures (8 °K), and even there the effect is quite small. This correction can be made fairly accurately using measurements on diamagnetic garnets, as discussed in I.

In general, phonons can introduce additional complications due to magnetoelastic effects.[33-35] However, we would expect these effects also to be very small in DAG since the crystal is extremely hard ($\Theta_D \sim 500$ °K) while the magnetic interactions are both weak and not very strain sensitive.[36] Additional experimental evidence that magnetoelastic effects are small was presented in I.

4. *Nuclear Effects*

Another effect which must be removed to isolate the intrinsic electronic properties is the contribution of the nuclear moments. There are seven stable Dy isotopes and two of them, Dy^{161} (18.9%) and Dy^{163} (25.0%), have nonzero nuclear spins. Both have spin $I = \frac{5}{2}$.[37] No detailed study of the hyperfine structure has been made specifically for DAG, but we can estimate the principal constants from experiments on other Dy compounds. In general we would expect an hyperfine interaction given by

$$\mathcal{H}_{\text{hyp}} = \sum_i \sum_{\alpha=x,y,z} A_\alpha^i S_\alpha I_\alpha + P_\alpha^i I_\alpha^2 , \tag{6}$$

where $\sum_\alpha P_\alpha = 0$ and where the magnetic hyperfine coefficients A_α^i are approximately proportional to the corresponding g values.[38,39] For DAG it is therefore a good approximation to neglect A_x^i and A_y^i. A_z^i can be determined from measured values of A/g for dysprosium acetate,[37] and we find

$$A_z^{161} = 72.0\times10^{-3} \text{ °K} ,$$

$$A_z^{163} = 100.9\times10^{-3} \text{ °K} .$$

For the case of Dy^{161}, this estimate can be checked against a direct Mössbauer-effect measurement[23] which gives

$$A_z^{161} = 73.9\times10^{-3} \text{ °K}$$

in reasonable agreement. The measurements also yield a value for $P_z^{161} = 5.3\times10^{-3}\,^\circ$K, making the reasonable assumption that P_x^{161} and P_y^{161} are small. Using the known ratio of the quadrupole moments,[37] this gives $P_z^{163} = -6.3\times10^{-3}\,^\circ$K, with P_x^{163} and P_y^{163} again small.

Combining these parameters we can estimate the contribution to the specific heat. (The effect on other magnetic properties will be negligible.) For a system which is essentially Ising-like, the hyperfine contribution can be calculated independently of the electronic interactions[40] and one can use the high-temperature expansion given by Bleaney.[41] For temperatures above 0.5 °K one thus finds

$$C_{hyp}/R = \sum_i x_i (b_i/T^2 + c_i/T^3 + \cdots) , \qquad (7)$$

where

$$b_i = \tfrac{35}{48}(A_z^i)^2 + \tfrac{56}{9}(P_z^i)^2$$

and

$$c_i = -\tfrac{14}{3}(A_z^i)^2 P_z^i + \tfrac{160}{27}(P_z^i)^3 ,$$

and x_i are the abundances of the isotopes. Substituting values, this gives

$$C_{hyp}/R = (2.8/T^2)\times10^{-3}(1 - 0.1/T + \cdots) . \qquad (8)$$

Compared with the electronic specific heat this is negligible above about 1 °K, but at the lowest temperatures the effect dominates the total specific heat. In this region an accurate correction for hyperfine effects is therefore important for estimating the small electronic contribution.

We shall show in Sec. IV that the expression given in Eq. (8) is in fact not completely adequate to yield the expected form for the electronic part, and we have therefore allowed for a possible variation in the coefficients in Eq. (8). Fitting the data with an effective hyperfine specific heat of the form b_{eff}/T^2 we find $b_{eff} = (3.1\pm0.3)\times10^{-3}$ (°K)^2 which is some 20% higher than the estimated value, and it is not clear at this time whether this is due to an error in the analysis, such as an error in the sign of P_i, or whether there is in fact some additional mechanism which contributes a specific heat of the order of $10^{-3}R/T^2$.[42] However, the effect is really quite small and it seems to be accounted for adequately by using the fitted value of b_{eff}.

While this allows for the nuclear effects in the region where they are relatively large, we should also consider the possibility of significant nuclear effects at higher temperatures, and in particular in the vicinity of the phase transition. The factorization of the partition function used to calculate nuclear effects independently of electronic interactions has been shown to be valid only for systems where both the electronic and hyperfine interactions have only z components.[40] This is certainly a very good approximation for DAG, but there are nevertheless small terms both of the kind $\mathcal{J}_{xx} S'_{xi} S'_{xj}$ and $A_x S'_x I_x$. It is possible, though it can be argued not very likely,[43] that cross terms between such interactions and the main z components could modify the overall magnetic behavior, especially in the region where intrinsic electronic properties diverge. Further theoretical study of this question would seem to be called for.

III. ASYMPTOTICALLY EXACT THEORIES

Having established the appropriate form for the effective spin-spin Hamiltonian [Eq. (3)], we are now in a position to derive theoretical expressions to compare with the observed data (corrected for the minor complications discussed above). Such expressions can readily be found in regions of "high" and "low" field and temperature using appropriate series expansions. The scale of "high" and "low" is set by three energies: $k_B T$, $g_e \mu_B H_0$, and $K_{ij} (\sim k_B T_N)$, and since the interactions cannot be treated exactly, we are generally restricted to regions where $k_B T \gg K_{ij}$ or $k_B T \ll K_{ij}$. In each of these regions one can readily derive partition functions for fields both low and high compared to $k_B T$, and one can thus find thermodynamic functions which are asymptotically exact as $k_B T$ and $g_e \mu_B H_0$ tend to zero or infinity.[44]

A. High-Temperature Zero-Field Specific Heat and Susceptibility

The method of series expansion in powers of $1/T$ for low fields is well known[45–47] and we shall follow the notation of Daniels.[47] The free energy F can be written in terms of the traces of powers of the interaction Hamiltonian (defined with $\mathrm{Tr}\,\mathcal{H} = 0$) as

$$F = -Nk_B T \ln 2 - k_B T\left(\frac{B}{T^2} + \frac{C}{T^3} + \frac{D - B^2/2}{T^4} + \frac{E - BC}{T^5} + \cdots\right) , \qquad (9)$$

where

$$B = \frac{\mathrm{Tr}(\mathcal{H}^2)}{2!\,k_B^2\,\mathrm{Tr}(1)} , \quad C = -\frac{\mathrm{Tr}(\mathcal{H}^3)}{3!\,k_B^3\,\mathrm{Tr}(1)} ,$$

$$D = \frac{\mathrm{Tr}(\mathcal{H}^4)}{4!\,k_B^4\,\mathrm{Tr}(1)} , \quad E = -\frac{\mathrm{Tr}(\mathcal{H}^5)}{5!\,k_B^5\,\mathrm{Tr}(1)} .$$

Differentiating with respect to T one obtains the entropy

$$S = -\frac{\partial F}{\partial T} = R\ln 2 - \frac{k_B B}{T^2} - \frac{2k_B C}{T^3} - \frac{3k_B(D - B^2/2)}{T^4} - \cdots \qquad (10)$$

and hence the specific heat for constant field, C_H, (which is equal to C_M for $H = 0$) is given by

$$C_H = T\left(\frac{\partial S}{\partial T}\right)_H$$

$$= k_B\left(\frac{2B}{T^2}+\frac{6C}{T}+\frac{12(D-B^2/2)}{T^4}+\cdots\right) . \quad (11)$$

Differentiating Eq. (9) twice with respect to H one obtains the zero-field susceptibility

$$\chi_0 = -\frac{\partial^2 F}{\partial H^2} = \frac{k_B}{T}\left(\frac{\partial^2 B}{\partial H^2}\right)+\frac{k_B}{T^2}\left(\frac{\partial^2 C}{\partial H^2}\right) + \frac{k_B}{T^3}\left[\frac{\partial^2}{\partial H^2}\left(D^2-\frac{B^2}{2}\right)\right]+\cdots . \quad (12)$$

Applying these expressions specifically to a system described by the Hamiltonian given in Eq. (3), one finds

$$S/R = \ln 2 - \theta_2/4T^2 - \theta_3/9T^3+\cdots , \quad (13)$$

$$C/R = \theta_2/2T^2+\theta_3/3T^3+\cdots , \quad (14)$$

and

$$\chi_0 = (\lambda/T)[1+\theta_1/T+(\theta_1^2-\theta_2)/T^2+\cdots] , \quad (15)$$

where

$$\theta_1 = \frac{-1}{k_B}\sum_j K_{ij} ,$$

$$\theta_2 = \frac{1}{k_B^2}\sum_j K_{ij}^2 ,$$

$$\theta_3 = \frac{-6}{k_B^3}\sum_{j>k} K_{ij}K_{jk}K_{ik} ,$$

and $\lambda = n_0 g_e^2 \mu_B^2/4k_B$. Here n_0 is the number of spins, and this is usually taken as Avogadro's number $N_0 = 6.025\times10^{23}$. λ is then the Curie constant per g atom of Dy^{3+}, which we may also call the Curie constant per mole, λ_M, since we are exclusively interested in the magnetic spins. For some purposes it is more convenient to use $n_0 = N_0/V_0$, where V_0 is the gram-atomic volume, and this gives λ_V, the Curie constant per unit volume. V can be calculated from the crystal structure[15-17] and is estimated to be 43.8 ± 0.2 cm^3.[48]

The form of Eqs. (13)–(15) will be valid quite generally, but the specific expressions for the θ's assume that all sites in the lattice are equivalent, so that any ion can be taken as the origin. In the case of θ_1, this is only valid for ellipsoidal sample shapes, since the K's always include some contribution from long-range dipolar interactions and the sum will be shape dependent. Since the shape dependence is really a macroscopic effect, it can be treated classically, and the values of θ_1 for two sample shapes defined by demagnetizing factors $N^{(A)}$ and $N^{(B)}$ are related by

$$\theta_1^{(A)}+\lambda_V N^{(A)} = \theta_1^{(B)}+\lambda_V N^{(B)} . \quad (16)$$

This is entirely equivalent to the usual relation between the susceptibilities

$$1/\chi_0^{(A)} - N^{(A)} = 1/\chi_0^{(B)} - N^{(B)} , \quad (17)$$

and it shows that if we reexpress Eq. (15) as a series for $1/\chi_0$ in powers of $1/T$, the entire shape dependence will appear in the constant term $-\theta_1/\lambda$:

$$1/\chi_0 = (T/\lambda)[1-\theta_1/T+\theta_2/T^2+\cdots] . \quad (18)$$

B. High-Temperature High-Magnetic-Field Specific Heat and Magnetization

The case of $k_B T \gg K_{ij}$ and arbitrarily high magnetic fields has been considered quite generally by Van Vleck.[45] Treating the magnetic field exactly (but always within the effective-spin approximation) one can evaluate the first- and second-order perturbations of the interactions, and hence derive a partition function from which the free energy can be found. The derivation is straightforward but somewhat tedious and we shall not give the details here[49-51] but simply quote the result for the free energy,

$$F/R = -T\ln\left[2\cosh\left(\frac{W}{kT}\right)\right]-\frac{\theta_1 t^2}{2} - \frac{2\theta_1^2 t^2(1-t^2)+\theta_2(1-t^2)^2}{4T} , \quad (19)$$

where $t = \tanh(W/k_B T)$, $W = g_e\mu_B H_0/2$, and $R = N_0 k_B$. Differentiating with respect to T we find the entropy and hence the specific heat at constant applied field:

$$C_{H_0}/R = (W/k_B T)^2 \operatorname{sech}^2(W/k_B T)[1+\delta_1+\delta_2] , \quad (20)$$

where

$$\delta_1 = \theta_1(k_B/W)[2t+(W/k_B T)(1-3t^2)]$$

and

$$\delta_2 = \theta_1^2(k_B/W)^2[t^2+4(W/k_B T)t(1-2t^2) + (W/k_B T)^2(1-9t^2+10t^4)] + \theta_2(k_B/W)^2[\tfrac{1}{2}(1-t^2)-4(W/k_B T)t(1-t^2) - (W/k_B T)^2(1-6t^2+5t^4)] .$$

The leading term in this expression is a simple Schottky anomaly corresponding to the splitting in the field, as we would expect. For zero field only the term δ_2 remains, and this reduces to $\theta_2/2T^2$ in agreement with the previous result [Eq. (14)].

Differentiating the expression for the free energy, Eq. (19), with respect to H we can derive a similar expression for the high-temperature magnetization:

$$M = M_0\tanh(W/k_B T)[1+\gamma_1+\gamma_2] , \quad (21)$$

where

$$\gamma_1 = (\theta_1/T)(1-t^2) ,$$

$$\gamma_2 = (\theta_1/T)^2(1-t^2)(1-2t^2)-(\theta_2/T)(1-t^2)^2 ,$$

and

$$M_0 = N_0 g_e \mu_B/2 .$$

In the absence of interactions this reduces to a

simple Brillouin function for $S' = \frac{1}{2}$ as it should, and in the limit as $H \to 0$ it reduces to the expression corresponding to the previously derived susceptibility [Eq. (15)].

C. Low-Temperature Zero-Field Specific Heat and Susceptibility

For low temperatures a different series-expansion technique must be used.[52] In general one must first determine the ground state and then calculate the energies of the possible elementary excitations and their statistical probabilities. For an Ising-like system very close to $T = 0\,^\circ\mathrm{K}$ this is very easy. The only elementary excitations are simple spin reversals, and if all sites are magnetically equivalent we can associate a single parameter Δ_0 with the excitation energy. The total internal energy at $T = 0\,^\circ\mathrm{K}$, U_0 is then related to Δ_0 by

$$-U_0 = \tfrac{1}{4} N \Delta_0 \,, \tag{22}$$

where half of the factor 4 comes from the usual self-energy and half from the fact that the energy to remove one spin from the ordered lattice costs only $\frac{1}{2}\Delta_0$. (As in I, we take the energy to the completely disordered state as zero.)

Corresponding to an energy gap Δ_0 the low-temperature specific heat is readily derived to be

$$\frac{C}{R} = (\Delta_0/k_B T)^2 \left(\exp \frac{\Delta_0}{k_B T} \right) \left(1 + \exp \frac{\Delta_0}{k_B T} \right)^{-2} , \tag{23}$$

as for a simple Schottky anomaly. As T increases, more complex excitations become probable, and a detailed analysis involving the microscopic structure is necessary to derive a form for C/R. However, we can proceed empirically and attempt to derive a value of Δ_0 from the measured data even in a range where Eq. (23) is no longer valid. If we define a temperature-dependent quantity $\Delta_{eff}(T)$ such that it reproduces the observed C/R when substituted in Eq. (23), we know that $\Delta_{eff} \to \Delta_0$ as $T \to 0\,^\circ\mathrm{K}$, and plotting $\Delta_{eff}(T)$ as a function of T one should therefore be able to extrapolate to find Δ_0. In practice it may be more accurate to plot Δ_{eff} against a more rapidly varying function of T which tends to zero with T, and in particular, we have found that plotting Δ_{eff} against C/R itself aids the extrapolation significantly.[53] We shall give the results of such an extrapolation in Sec. IV, but we shall defer until Paper IV a discussion of the relationship between Δ_0 and the individual K_{ij} in Eq. (3).

The same sort of analysis can be applied to the low-field susceptibility. If the ground state is antiferromagnetic the moment in a weak field is directly proportional to the number of spin excitations, and this in turn is proportional to $\exp(-\Delta_0/k_B T)$. The susceptibility as T tends to zero is thus given by

$$\chi_0 = (\lambda/T) \exp(-\Delta_0/k_B T) \,. \tag{24}$$

We may note that this result appears to be independent of sample shape, in contradiction in our usual ideas, but this paradox is resolved if we recall that Eq. (24) is strictly valid only as $T \to 0$, where $\chi \to 0$, so that the demagnetizing field vanishes as well. At finite temperatures the asymptotic form must be modified and we can proceed as in the case of the specific heat by defining a $\Delta_{eff}(T)$.

The potential accuracy of both these methods of estimating Δ_0 is quite good because errors in the absolute values of C/R or χ have relatively little effect on the fitted value of Δ_{eff}. For example, if the true specific heat C_1/R is characterized by Δ_1 while the experimental specific heat C_2/R corresponds to Δ_2, then

$$\frac{C_1}{C_2} = \left(\frac{\Delta_1}{\Delta_2} \right)^2 \exp\left(\frac{\Delta_2 - \Delta_1}{k_B T} \right)$$

$$\approx \left(\frac{\Delta_1}{\Delta_2} \right)^2 \left(1 + \frac{\Delta_2 - \Delta_1}{k_B T} + \cdots \right) \tag{25}$$

for $\Delta_2 - \Delta_1 \ll k_B T$. If we express the error in C as $x = (C_2 - C_1)/C_1$ we can express the corresponding error in Δ, $\delta = (\Delta_2 - \Delta_1)/\Delta_1$, in terms of x. For small x and δ this gives

$$\delta = \frac{x}{\Delta_2/T - 2} \,. \tag{26}$$

The ratio Δ_2/T is typically 5 to 10, so that even a 5% error in C leads to an error of less than 1% in Δ_{eff}. Even so, care must be taken in applying this method, since it involves using measurements of C and χ where both are necessarily very small and thus especially sensitive to systematic errors such as an incorrect subtraction of nuclear effects or the temperature-independent paramagnetism.

D. Low-Temperature High-Field Specific Heat and Magnetization

The same general method can be used for handling high fields and low temperatures. The ground state is now the fully magnetized configuration, $\sigma_i = -1$ for all i, and the lowest elementary excitations are again single spin flips. In the absence of interactions, the energy of these excitations is $g_e \mu_B H_0$ and including interactions this is changed to

$$\Delta_0(H_0) = g_e \mu_B (H_0 + h_i)$$

$$= g_e \mu_B H_0 + \Delta_0' \,, \tag{27}$$

where Δ_0' is a constant independent of H_0. In fact Δ_0' can be related very simply to the interaction constants in Eq. (3) since the reversal of a single spin from the ground state clearly involves an energy

$$\Delta_0' = -2 \sum_j K_{ij} \,, \tag{28}$$

where we assume, as before, that all sites are equivalent. Thus Δ_0' is directly proportional to the "high-temperature" parameter θ_1 defined in Eq. (15),

$$\Delta_0' = 2k_B\theta_1 , \tag{29}$$

and it will reflect the same shape dependence.

Both Δ_0' and θ_1 may be interpreted very simply in terms of mean field theory which becomes asymptotically exact at very high temperatures in all cases and at very low temperatures in the case of an Ising-like system. In mean field theory the effect of the interactions from neighboring spins is replaced by a field $H_M(0)\cdot(M/M_0)$ and at high temperatures this leads to the usual Curie-Weiss law, with

$$\theta = \theta_1 = [H_M(0)/M_0]\lambda = H_M(0)(g_e\mu_B/2k_B) .$$

At low temperatures and high fields $M/M_0 \to 1$ and the internal field tends to $H_M(0)$. The energy of reversing a single spin in this field is $g_e\mu_B H_M(0) = \Delta_0'$ and hence $\Delta_0' = 2k_B\theta_1$, as before.

The low-temperature specific heat in a field follows directly from Eq. (23) with Δ_0 replaced by $\Delta_0(H_0)$, and we can use the same procedure of defining a $\Delta_{\text{eff}}(H_0, T)$ and extrapolating to $T = 0\,^\circ$K. The resulting values of $\Delta_0(H_0)$ should vary linearly with H_0 and the slope should be proportional to g_e. Since g_e is already well determined from other experiments this provides a useful check in the present case, but it could, in principle, be used as an independent determination of g_e.[54]

The low-temperature magnetization can be obtained similarly by considering single-spin reversals as the excitations above the fully magnetized state. The probability of an excitation with energy $\Delta_0(H_0)$ is simply given by the Boltzmann factor, $e^{-x}/(1+e^{-x})$ with $x = \Delta_0(H_0)/k_BT$, and the moment associated with each excitation is $g_e\mu_B$, so that the total moment is given by

$$\begin{aligned} M &= N_0 g_e\mu_B\,(1-e^{-x})/2(1+e^{-x}) \\ &= M_0 \tanh[\Delta_0(H_0)/2k_BT] \end{aligned} \tag{30}$$

as we might expect. If the sum of the interactions in the aligned state is small, i.e., $\Delta_0' \ll g_e\mu_B H_0$, this expression again reduces to the simple Brillouin function for $S' = \frac{1}{2}$. This in fact turns out to be the case for DAG in fields above a few kOe, and one should therefore be able to estimate M_0 by evaluating $M/\tanh(g_e\mu_B H_0/2k_BT)$ and extrapolating to high fields.

However, before this can be done it is necessary to take into account the temperature-independent contributions to M discussed in Sec. II C 2. These simply add a term $m = \chi_{VV}(H_0 + aM)$, Eq. (5), and the high-field asymptote of $y = M/\tanh(g_e\mu_B H_0/2k_BT)$ plotted as a function of H_0 is thus not a constant, but is given by

$$y = M_0(1 - a\chi_{VV}) + \chi_{VV}H_0 . \tag{31}$$

The slope of this line immediately gives χ_{VV}, while the intercept gives $M_0(1 - a\chi_{VV})$ where the constant a can be estimated as discussed in Sec. II C 2. For DAG the correction term $a\chi_{VV}$ turns out to be very small (~ 0.0019) but for other systems the induced moment could well be much larger.

E. Phase Transition at $T = 0\,^\circ$K

The zero-field ground state of an Ising antiferromagnet is unaffected by magnetic fields and since there is a finite energy gap to excited states, it will completely dominate the low-field properties as $T \to 0\,^\circ$K. At higher fields, on the other hand, one or more of the excited states will be depressed in energy by the field until one of them becomes the new ground state, and at $T = 0\,^\circ$K this will manifest itself as an abrupt (first-order) phase transition as the field is increased. In a simple two-sublattice system there is only one such transition, corresponding to the crossing of the fully saturated state ($M = M_0$) with the ground state, and we denote the field for this condition by $H^c(0)$. This field can be estimated by extrapolation of the $H^c(T)$ vs T phase diagram determined at finite temperatures, as will be described in Sec. IV B 4.

$H^c(0)$ is readily related to parameters already discussed above. The transition will occur when the free energies of the two states become equal, but at $T = 0\,^\circ$K this is equivalent to equating the spectroscopic energies. The zero-field energy is given in terms of Δ_0 by Eq. (22) and the energy in a large field, E_H, is likewise related to $\Delta_0(H_0)$ and Δ_0' by

$$\begin{aligned} E_{H_0} &= -\tfrac{1}{2}N_0 g_e\mu_B(H_0 + \tfrac{1}{2}h_i) \\ &= -\tfrac{1}{2}N_0[\Delta_0(H_0) - \tfrac{1}{2}\Delta_0'] \\ &= -M_0H_0 - \tfrac{1}{4}N\Delta_0' , \end{aligned} \tag{32}$$

where the factor $\frac{1}{2}$ multiplying h_i and Δ_0' again reflects the difference in counting energies in applied and internal fields. Equating $U_0\,(\equiv E_{H=0})$ with $E_{H_0 = H^c(0)}$ we thus find

$$H^c(0) = (\Delta_0 - \Delta_0')/2g_e\mu_B . \tag{33}$$

Throughout this discussion we have assumed implicitly that all spins in the sample will behave in a similar manner, but this is in fact only true if we have no domains. As discussed in some detail by Wyatt[55] and also in I this is the case only for a sample with no demagnetizing field, e.g., a long thin needle, and Eq. (33) thus applies directly to the *internal* critical field $H_i^c(0)$. Correspondingly, the value of Δ_0' in Eq. (33) must be that appropriate to a shape with zero demagnetizing factor and it must be related to estimates of Δ_0' or θ_1 made on other shapes using Eqs. (16) and (29).

F. Application of Asymptotic Expressions

It should be emphasized again that the expressions

derived in the previous sections are only *asymptotically exact* and that care must be taken in comparing them with experimental data taken in some particular region of H and T. However, given proper care the expressions can in fact be extremely useful, in that they allow a large amount of experimental information to be reduced to a relatively small set of characteristic parameters, which can then be related directly to a microscopic Hamiltonian such as Eq. (3).

IV. ANALYSIS OF EXPERIMENTAL RESULTS

A. Determination of Single-Ion and Collective Parameters

The theoretical expressions derived above contain four single-ion parameters (g_e, M_0, λ, and χ_{VV}) and six collective parameters [θ_1, θ_2, θ_3, Δ_0, U_0, $H^c(0)$] and we shall now determine values of these using the experimental data given previously in I. The parameters are of course not independent, and a number of cross checks are therefore possible which test both the consistency of the experimental data and the theoretical assumptions. We shall discuss this consistency in more detail in Paper IV, and for the present we will concentrate on using each type of measurement to extract the best values for the corresponding parameters involved in the theoretical expressions. A brief discussion of some of the simpler correlations which can immediately be made is given in Sec. IV A 9 below, which also includes two tables summarizing the single-ion and collective parameters determined in this work and in earlier publications.

1. High-Temperature Zero-Field Specific Heat

The specific heat corresponding to the effective spin-spin interactions C_M was obtained from the measured total by subtracting estimates for the sample holder, the lattice contribution, and the Schottky tail due to the level of E_1, as described in Paper I and Secs. II and III above. The results are shown in Fig. 1, in which $C_M T^2/R$ is plotted as a function of $1/T$. It can be seen that the errors become quite large at the highest temperatures and that there is some uncertainty in the extrapolation of the curve to $1/T = 0$. Even so, we can obtain a fairly good estimate of the intercept and a rough estimate of the initial slope, and using Eq. (14) we find

$$\theta_2 = (3.5 \pm 0.4)\ (^\circ\mathrm{K})^2$$

and

$$\theta_3 = (5.1 \pm 3.0)\ (^\circ\mathrm{K})^3 .$$

The rather large error limits on θ_3 reflect an additional uncertainty due to the possibility that the next term in the series may not be entirely negligible, but the experimental results are clearly not accurate enough to determine this. These results are also in good agreement with recent high-frequency relaxation measurements of C_M which give[56]

$$\theta_2 = (3.7 \pm 0.2)\ (^\circ\mathrm{K})^2 ,$$

$$\theta_3 = (6.0 \pm 2.7)\ (^\circ\mathrm{K})^3 .$$

We can use these values to estimate the contributions to the entropy and the internal energy from the temperature region above that over which direct measurements were made, and these estimates may be used to relate S/R and U/R to appropriate zeros, as described in I. We thus find

$$\frac{\Delta S}{R}\bigg|_{T=8^\circ\mathrm{K}}^{T=\infty} = \int_8^\infty \frac{C}{RT}\,dT = 0.016 \pm 0.002 \tag{34}$$

and

$$\frac{\Delta U}{R}\bigg|_{T=8^\circ\mathrm{K}}^{T=\infty} = \int_8^\infty \frac{C}{R}\,dT = 0.23 \pm 0.03 , \tag{35}$$

which are the values used in I.

2. High-Temperature Zero-Field Susceptibility

An accurate analysis of the high-temperature susceptibility in terms of the interactions is much harder than for the specific heat, since the susceptibility is dominated by the leading Curie-law term while the interactions contribute only to the

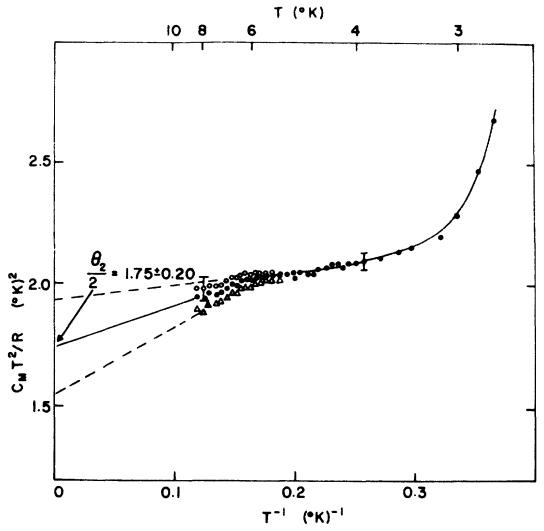

FIG. 1. High-temperature zero-field magnetic specific heat of DAG, plotted as $C_M T^2/R$ as a function of T^{-1}. The three sets of experimental points, denoted by ○, △, and •, represent the extreme limits and the best estimate for the lattice and Schottky contributions which must be subtracted from the total specific heat to obtain C_M. Typical experimental uncertainties in the measured total specific heat are indicated by the error bars. Extrapolation to $T^{-1} = 0$ determines the asymptotic behavior of the form $C_M T^2/R = \frac{1}{2}\theta_2 + \frac{1}{3}\theta_3/T$, with $\theta_2 = 3.5 \pm 0.4$ (°K)^2 and $\theta_3 = 5.1 \pm 3.0$ (°K)^3.

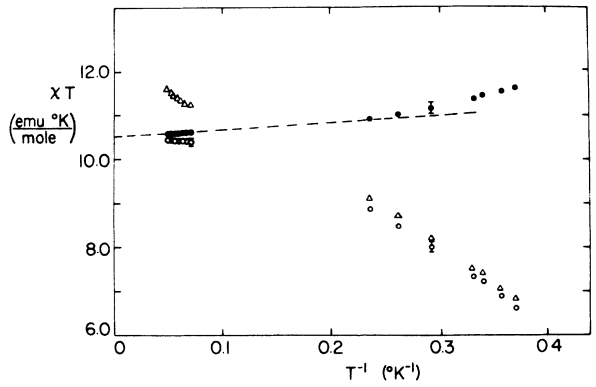

FIG. 2. Analysis of high-temperature susceptibility of DAG, showing effect of temperature-independent contribution χ_{VV} and higher-order interaction terms in the series expansion [Eq. (15)]. $\Delta\Delta\Delta = \chi T$ as measured on a spherical sample (after Refs. 6 and 55); ooo $= (\chi - \chi_{VV})T$ with $\chi_{VV} = 0.054$ emu/mole; ●●● $= (\chi - \chi_{VV})T - \lambda(\theta_1^2 - \theta_2)/T^2$ with $\lambda = 10.3$ emu °K/mole; $\theta_1 = 0.2$ °K and $\theta_2 = 3.5$ (°K)^2; --- = estimated high-temperature asymptote corresponding to $\lambda = 10.45 \pm 0.15$ emu °K/mole; $\theta_1 = (+0.20 \pm 0.15)$ °K.

higher-order terms. Moreover, the effect of the temperature-independent susceptibility can be quite significant and care must be taken to ensure that the various competing terms are taken into account properly. In this respect DAG is no different from many other magnetic systems,[57] but our ability to cross check specific parameters with independent determinations makes it possible in the present case to make proper allowance for these complications.

High-temperature susceptibility results extending up to 20 °K have been reported by Ball *et al.*,[6] but these measurements were made on a loosely packed powder sample and it was therefore not possible to apply an accurate correction for demagnetizing effects. However this correction can be estimated quite accurately by comparing the powder values of $1/\chi$ with corresponding values obtained by Wyatt[55] for a spherical single crystal at temperatures below 4.2 °K. In the region over which the two sets of data overlap there is an essentially constant difference, and using Eq. (17) one can estimate the effective value of N for the powder sample. This value can then be used to correct the powder susceptibility to that corresponding to a 100% dense spherical sample. In Fig. 2 we plot as triangles the values of $\chi_{\text{sphere}} T$ as obtained in this way as a function of T^{-1} and it can be seen that the results appear to fall quite close to a straight line, as might be expected from Eq. (15) if the first two terms were dominant. However, if this were the case, the line would imply a Curie constant of about 12.2 emu °K/mole and this is significantly larger than the value 10.3 ± 0.2 emu °K/mole calculated from the g values determined from optical, thermal, and high-field magnetization measurements. It is clear therefore that a naive analysis of χ gives a completely wrong result in the present case.

To resolve the discrepancy, we note first that the high-field magnetization results give a direct measure of the Van Vleck temperature-independent susceptibility (see Sec. IV A 3 below), which though small (0.054 emu/mole) is significant. Before one can apply Eq. (15) one must of course subtract the temperature-independent contribution, and the result of this subtraction is shown by the open circles in Fig. 2. It can be seen that the extrapolation to $T^{-1} = 0$ now gives a value for the Curie constant much closer to our independent estimate, but there is now a significant amount of curvature as T^{-1} increases, in contrast to the previous straight line!

This suggests that the third- (and possibly higher-) order terms in Eq. (15) are in fact not negligible and this is confirmed by our previous estimates of θ_2 and θ_3 (see Sec. IV A 1 above). Since the higher-order coefficients in the expansion of χ cannot be obtained simply, we will only use the term $(\theta_1^2 - \theta_2)$ to estimate their effect, and in Fig. 2 we show by the filled circles the result of plotting

$$\chi' T = (\chi_{\text{sphere}} - \chi_{VV})T - \lambda(\theta_1^2 - \theta_2)/T^2$$

as a function of T^{-1}, with $\theta_2 = 3.5$ (°K)^2, $\lambda = 10.3$ emu °K/mole, and $\theta_1 = 0.2$ °K as determined self-consistently from the final result. It can be seen that there is now curvature only at the lowest temperatures, due primarily to the neglected higher-order terms in the series. These will presumably have only a small effect on the points in the range $T^{-1} = 0.05$ to 0.07 (°K)$^{-1}$ and we can therefore obtain a reasonably good estimate of the high-temperature asymptote from these points. This is shown by the broken line in Fig. 2 and it corresponds to

$$\lambda_M = 10.45 \pm 0.15 \text{ emu °K/mole},$$

$$\theta_1 = (+0.20 \pm 0.15) \text{ °K},$$

where the error limits include the uncertainties in the corrections due to χ_{VV} and θ_2 as well as in the experimental data. The small value of θ_1 is quite remarkable and it will be confirmed by other measurements (see Secs. IV A 7 and IV A 8). It arises from an unusual cancellation of the interactions between otherwise equivalent neighbors due to the predominantly dipolar nature of the interactions and the complex structure of the garnet lattice. We shall discuss this further in Paper IV.

3. *High-Temperature High-Field Magnetization*

The same sorts of difficulties complicate the analysis of the magnetization in higher fields and in practice no useful parameters can be extracted from these data although they are generally consistent

with Eq. (21) and the parameters already derived. However, the form of the field variation predicted by Eq. (21) is interesting in that it explains the previously noted bump in $(\partial M/\partial H_0)_T$ as a function of field[1] at temperatures between 2.5 and 3.8 °K. If we simplify Eq. (21) by taking $\theta_1 = 0$, the term in γ_2 indicates a depression of the magnetization curve below the ideal Brillouin function for $S' = \frac{1}{2}$, but as the field increases $t \to 1$ and the whole term tends to zero corresponding to a relative increase in M. This can give rise to an inflexion in the M vs H curve and hence a bump in $(\partial M/\partial H_0)_T$. No attempt has been made to analyze this effect in detail as it appears to be an essentially trivial result arising from the particular relation of θ_1, θ_2, and $g_e\mu_B H_0$. However it is interesting to note that such a variation could not have been predicted on the basis of mean field theory, so that the effect is intrinsically a result of short-range order.

4. *High-Temperature High-Field Specific Heat*

Specific-heat measurements in magnetic fields have only been made up to 4.2 °K and we would really not expect the asymptotic high-temperature form of Eq. (20) to be valid quantitatively at this temperature. However, we may note that the correction terms δ_1 and δ_2 become progressively less important as H_0 increases, so that we might hope that the asymptotic form would fit the results for the highest fields quite closely, at least near the upper end of the measured temperature range.

The results of measurements at 14.33 kOe taken from I are shown in Fig. 3, and it may be seen that the curve does indeed follow an unmodified Schottky anomaly corresponding to $\delta_1 = \delta_2 = 0$ quite closely. To allow for the interactions we fitted Eq. (20) under several constraints and this provides some insight into the accuracy with which the parameters can be determined.

When all of the data points between 1 and 4.2 °K were included, both the convergence of the fit and the final standard deviation were poor. However when only the points above 2.5 °K were included, the convergence was rapid and yielded $g_e = 11.1$, $\theta_1 = -0.57$ °K, and $\theta_2 = 4.1$ (°K)^2. Constraining θ_2 to the value previously found from the zero-field specific heat, $\theta_2 = 3.5$ (°K)^2, a good fit for g_e and θ_1 could again be obtained, this time yielding $g_e = 10.8$ and $\theta_1 = -0.46$ °K. Repeating this procedure but including only data points above 3.0 °K gave $g_e = 10.2$, $\theta_1 = -0.23$ °K, and $\theta_2 = 2.0$ (°K)^2 with all three parameters allowed to vary, and it gave $g_e = 10.8$ and $\theta_1 = -0.47$ °K with θ_2 again fixed at 3.5 (°K)^2. The calculation corresponding to these parameters is shown as the solid curve in Fig. 3. When more points were deleted from the low-temperature part of the curve the fitted parameters fluctuated with the number of data points, showing that scatter in the data was becoming important and that fits to the remaining data points were not meaningful.

From this analysis we can conclude that the high-temperature specific heat in a field of 14.33 kOe is represented quite well by Eq. (20) with

$$g_e = 10.6 \pm 0.5,$$

$$\theta_1 = (-0.4 \pm 0.3)\ °\mathrm{K},$$

$$\theta_2 = 3.1 \pm 1.0\ (°\mathrm{K})^2,$$

where the errors have been estimated to allow for the limitations in the analysis as well as experimental uncertainties. All three results are generally consistent with other determinations of the same parameters but, as we might expect, the accuracy of several alternative methods is intrinsically higher.

In comparing the value of θ_1 with other results we must note that θ_1 will be shape dependent and that the present value applies to a sample with demagnetizing factor $N = 5.35$. Using Eq. (16) we can calculate the corresponding value for a sphere and find $\theta_1^{\mathrm{sphere}} = -(0.13 \pm 0.30)$°K, confirming again the unusually small value of $\theta_1^{\mathrm{sphere}}$.

5. *Low-Temperature Zero-Field Specific Heat*

An early analysis of specific-heat measurements down to 1.3 °K by Ball *et al.*[58] has given a value for the energy gap $\Delta/k_B = 7.2$ °K, but at these temperatures the excitation of multiple spin flips is not entirely negligible and we might expect the fitted Δ_{eff} to differ somewhat for the true Δ_0. We have therefore extended the measurements down to 0.5 °K, as described in I, and this range should

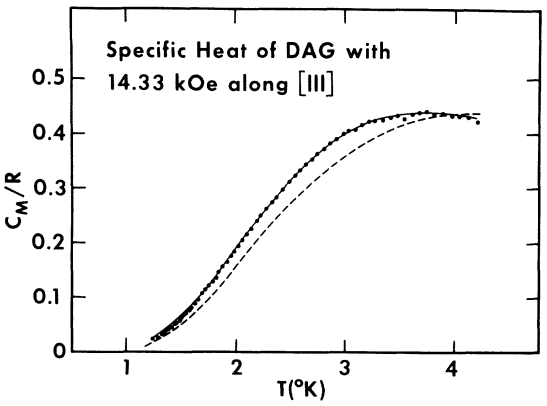

FIG. 3. Comparison between the measured and calculated magnetic specific heat of DAG in a field of 14.33 kOe applied along [111]. ●●● = measured specific heat (lattice and hyperfine contributions negligible) after Ref. 1; --- = calculated for no interactions [Eq. (20) with $\delta_1 = \delta_2 = 0$ and $g_e = 10.6$]; ——— = calculated curve including interactions to second order [Eq. (20)] with $\theta_1 = -0.47$ °K, $\theta_2 = 3.5$ (°K)^2, and $g_e = 10.8$.

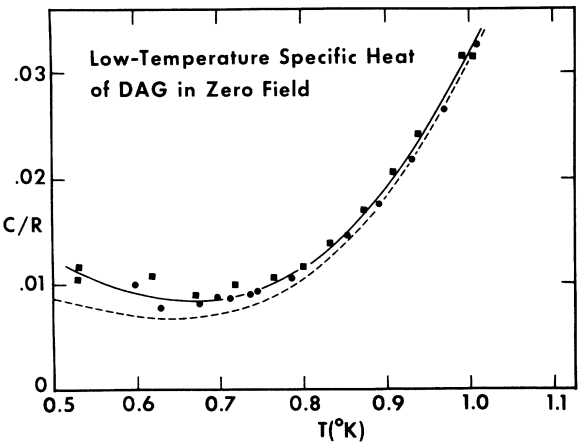

FIG. 4. Low-temperature zero-field specific heat of DAG compared with theory including hyperfine interaction and the effect of low-lying spin excitations. ▪ and ● = experimental points (after Ref. 1); --- = calculated variation [Eqs. (7) and (23)] using the hyperfine parameters estimated in Eq. (8) and $\Delta_0/k = 7.60$ °K; ——— calculated variation using an empirically fitted hyperfine contribution $C_{hyp}/R = (3.1 \times 10^{-3})/T^2$ and $\Delta_0/k = 7.60$ °K.

certainly be low enough to give the correct asymptotic value without any further extrapolation.

However, we first have to isolate the true electronic specific heat, and this entails a sizable correction for nuclear effects. In principle this should be straightforward and we can use the estimate discussed in Sec. II C 4, which we might expect to be quite accurate (±5%, say). However, when we used a correction of the magnitude of Eq. (8) we found that the remaining specific heat did not in fact go to zero as it should, so that we must conclude that the correction used was not quite big enough. This could arise either from a systematic error in the measurements of the specific heat, which is very small in this region, or from an error in the analysis of the nuclear effects, or from an additional mechanism such as a magnetic impurity, which could also give a $1/T^2$ specific heat in this region. The effect is quite small and the simplest solution is to treat the total nonelectronic correction in terms of a single adjustable constant b_{eff}/T^2 and to fit b_{eff} to the data together with Δ_0. The possible error in such a procedure is likely to be quite small especially in the region 0.7–1.0 °K where the total correction is quite small.

The results of such a fit are shown in Fig. 4, and it can be seen that the agreement is indeed very good over the whole range. The corresponding parameters are

$$\Delta_0/k_B = (7.60 \pm 0.05)\ ^\circ\mathrm{K}$$

and

$$b_{eff} = (3.1 \pm 0.3) \times 10^{-4}\ (^\circ\mathrm{K})^2 .$$

The difference between this value of Δ_0 and the earlier estimate is in the direction we might expect, inasmuch as the neglect of multiple excitations will generally increase the specific heat and thus lead to smaller value of Δ_{eff}. The value is also in excellent agreement with optical determinations[10,11] and this agreement provides additional evidence for the validity of the Ising-model approximation. We shall discuss this point further in Paper IV.

6. *Low-Temperature Low-Field Magnetization and Susceptibility*

As discussed in I, the low-field magnetization leads to a zero-field susceptibility χ_0 which agrees with direct ac measurements, and we can analyze the temperature variation of this using Eq. (24). However, we must first subtract the ubiquitous temperature-independent susceptibility χ_{VV}, and for this we again use the value 0.054 emu/mole obtained from the high-field data (Sec. IV A 7). Fitting $\chi_0 - \chi_{VV}$ to Eq. (24), we obtain a series of values of $\Delta_{eff}(T)$ and these are shown in Fig. 5, where we plot $\Delta_{eff}(T)$ as a function of $\chi_0 - \chi_{VV}$. As explained before, this type of plot should be better than a direct plot against T for extrapolating Δ_{eff} to $T = 0$ °K, and it leads to an intercept

$$\Delta_0/k_B = (7.54 \pm 0.06)\ ^\circ\mathrm{K},$$

in excellent agreement with the values derived previously. The close agreement, especially for the points at the lowest temperatures, shows that the estimate of χ_{VV} is essentially correct since χ_0 becomes equal to $2\chi_{VV}$ at about 1.2 °K.

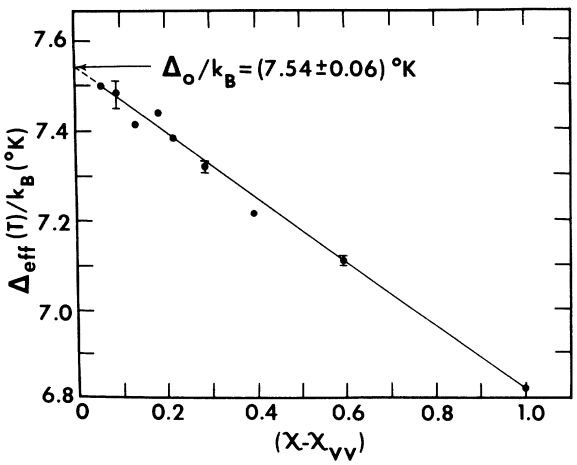

FIG. 5. Determination of low-temperature energy gap of DAG in zero field from measurements of the differential susceptibility. $\Delta_{eff}(T)$ calculated from measured values of χ_0 using Eq. (24). Extrapolation to $\chi_0 - \chi_{VV} = 0$ (equivalent to $T = 0$ °K) gives $\Delta_0/k_B = (7.54 \pm 0.06)$ °K.

TABLE I. Saturation magnetization and Van Vleck temperature-independent paramagnetism from analysis of isothermal magnetization curves.

T(°K)	M_0(emu/cm^3)	χ_{VV}(10^4 emu/cm^3)
1.138	667.2	12.7
1.254	666.4	12.2
1.355	666.0	12.3
1.464	665.4	12.7
1.506	665.4	11.4
1.600	667.1	12.4
Average	666.2	12.3

7. *Low-Temperature High-Field Magnetization*

The high-field magnetization is readily analyzed using Eq. (31). At each temperature we plot $M/\tanh(g_e\mu_B H_0/2k_B T)$ as a function of H_0 and determine the slope and intercept of the straight lines to which the plots become asymptotic. Using the correction $(1-a\chi_{VV})$ discussed before, this leads to the results shown in Table I. It can be seen that there is no systematic variation of either M_0 or χ_{VV}, showing that the method of extrapolation is valid, and taking the average we conclude that

$$M_0 = 666 \pm 4 \text{ emu/cm}^3$$

and

$$\chi_{VV} = (12.3 \pm 1.0) \times 10^{-4} \text{ emu/cm}^3,$$

where the error limits include estimates of systematic errors. Using the value $V = 43.8$ cm^3 for the gram-atomic volume these results may also be expressed as

$$M_0 = (2.90 \pm 0.02) \times 10^4 \text{ emu/mole},$$

corresponding to $(5.19 \pm 0.04)\mu_B$/atom, and

$$\chi_{VV} = (5.4 \pm 0.4) \times 10^{-2} \text{ emu/mole},$$

where 1 mole is again understood to denote N_0 ions of Dy^{3+}. This estimate of χ_{VV} may be compared with the value 6.2×10^{-2} emu/mole previously determined for 5% Dy^{3+} in diamagnetic YAG.[6] The small difference is readily explained by the somewhat smaller crystal-field splittings found in the diluted system.[8,10,12,14] As we shall see later, the result for M_0 is in excellent agreement with a number of other determinations of the effective magnetic moment.

8. *Low-Temperature High-Field Specific Heat*

The specific heat in high magnetic fields may be analyzed in the same way as the zero-field specific heat. If one uses only measurements above about 1.2 °K one can neglect the nuclear contributions, but it is then necessary to extrapolate the fitted values of Δ_{eff} to obtain the correct $\Delta_0(H_0)$. Alternatively one can use the available data down to 0.5 °K and assume that Δ_{eff} is approximately equal to Δ_0 in this range, but one must then fit a value of b_{eff} for the hyperfine and other low-temperature contributions. We have used both methods and it is of interest to compare the results.

In Fig. 6 we plot the values of $\Delta_{eff}(T)/k_B$ corresponding to an applied field of 14.33 kOe as a function C/R, and it can be seen that the asymptotic value is reached for $C/R < 0.06$. This value is (9.82 ± 0.05) °K and this can be compared with the value of $g_e\mu_B H_0/k_B = 10.1$ °K which would correspond to a simple Schottky tail with zero interactions. The small negative difference indicates that θ_1 is quite small and antiferromagnetic, but we shall defer extracting value for θ_1 until we have analyzed some of the other results.

Measurements in various fields between 8 and 14 kOe were made down to 0.5 °K as reported in I, and these were fitted to expressions of the form

$$\frac{C_{H_0}}{R} = \left(\frac{\Delta_{eff}(H_0)}{k_B T}\right)^2 \exp\left(-\Delta_{eff}(H_0)/k_B T\right) + \frac{b_{eff}}{T^2} \tag{36}$$

for each value of H_0. To ensure that this asymptotic form should be valid, only values of $C/R < 0.06$ were used, as indicated by the results shown in Fig. 6. The resulting values of $\Delta_0(H_0)$ are plotted as a function of H_0 in Fig. 7. It can be seen that the results lie on a good straight line which has an intercept close to but not at the origin. From the slope of the line we can get a value of g_e,

$$g_e = 10.6 \pm 0.2,$$

and from the intercept we get

$$h_i = -670 \pm 200 \text{ Oe},$$

which corresponds to

$$\Delta_0'/k_B = 2\theta_1 = (-0.470 \pm 0.140) \text{ °K}.$$

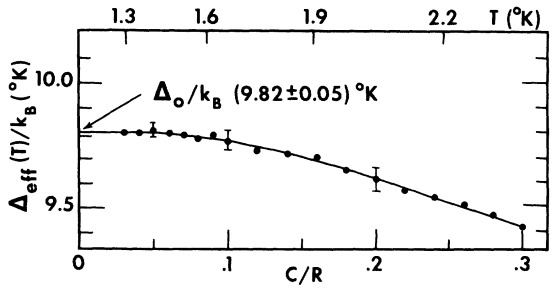

FIG. 6. Variation of $\Delta_{eff}(T)/k_B$ with T for DAG in a field of 14.33 kOe applied along [111], as calculated from specific-heat measurements using Eq. (23). The asymptotic value which is found for $C/R < 0.06$ is (9.82 ± 0.05) °K. This may be compared with $g_e\mu_B H_0/k_B = (10.1 \pm 0.2)$ °K which would be expected if there were no interactions, taking $g_e = 10.5 \pm 0.2$.

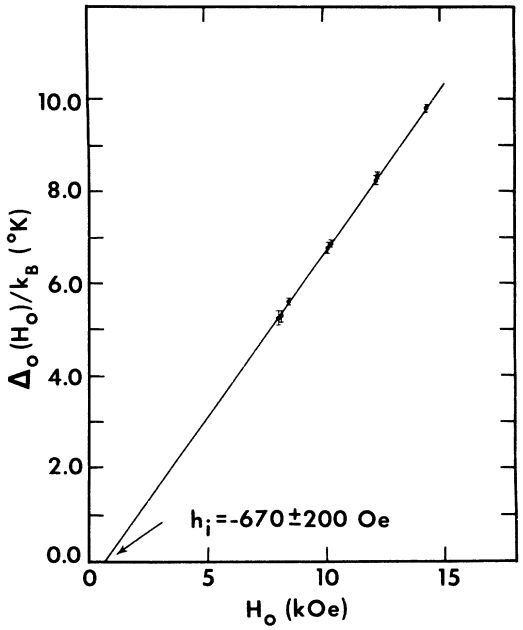

FIG. 7. Low-temperature energy gap $\Delta_0(H_0)$ for DAG in applied fields along [111]. The straight line represents the best fit corresponding to $\Delta_0(H_0) = g_e\mu_B(H_0 + h_i)$, with $g_e = 10.6 \pm 0.2$ and $h_i = -670 \pm 200$ Oe. The intercept h_i is related to θ_1 [see Eqs. (27) and (29)] and after applying a correction for shape (Eq. 16) it gives $\theta_1^{\text{sphere}} = (0.04 \pm 0.07)$ °K.

As before, this value corresponds to an ellipsoid with $N = 5.35$, and using Eq. (16) to correct the value to that of a sphere we get

$$\theta_1^{\text{sphere}} = (0.04 \pm 0.07)\ ^\circ\text{K}.$$

The fitted values of b_{eff} showed no field dependence and gave an average value $b_{eff} = (3.3 \pm 0.5) \times 10^{-3}$ (°K)^2, in good agreement with the value determined in zero field. The fact that b_{eff} does not vary significantly with H_0 suggests that the difference from the calculated value of $2.8\ (1 - 0.1/T) \times 10^{-3}$ (°K)^2 may perhaps be due to systematic errors in either the experiment or the analysis and not due to magnetic impurities, but at the moment we are not able to resolve this question.

In any case there is no doubt that θ_1^{sphere} is again determined to be very small and that g_e is close to the value we find from other data (see Sec. IV A 4).

9. *Summary of Single-Ion and Collective Parameters*

The parameters determined in the previous sections are summarized in Tables II and III, which include also corresponding values reported in the literature. It may be seen that there is generally good agreement between the many experiments which have been performed on DAG. We shall defer a discussion of the collective parameters until Paper IV since this will involve the details of the interaction Hamiltonian, but we can readily correlate some of the single-ion parameters using the discussion already given here.

In particular, if we assume that g_x^2 and g_y^2 are small compared to g_z^2, we can relate the empirically determined values of g_e to g_z using Eq. (1), and we can then also relate λ and $M_0(111)$ to g_z using Eqs. (15) and (21). The values of g_z derived in this way are shown in Table II and it can be seen that they are in excellent agreement with the more direct determinations using fields applied along one of the local z axes. All the variable data are thus seen to be consistent with the conclusion that the g tensor in DAG is indeed very highly anisotropic, as has been assumed for some time.

The collective parameters can be checked in a purely empirical way, since we have several independent determinations of each of the quantities $\Delta_0, H_{111}^c(0)$, θ_1, and θ_2. We again find generally good consistency, lending support to both the experimental results and the general method of analysis. The relationship of these four parameters to a microscopic Hamiltonian of the form given in Eq. (3) will be discussed in Paper IV.

B. Determination of Critical Parameters

The parameters characterizing the phase transition from the paramagnetic to the antiferromagnetic state are quite different from the single-ion and collective parameters discussed in Sec. IV A. The latter are related by expressions which are asymptotically exact, and the statistical approximations depend on the model Hamiltonian in a very direct way. The critical parameters on the other hand generally imply very profound statistical approximations and it is by no means trivial to relate most of them to our model Hamiltonian. However, it seems appropriate to extract a number of such parameters from the data at this time so as to provide a well-defined basis for further theoretical work on DAG. We can identify four characteristic regions on the phase diagram as we shall consider each in turn.

1. *Zero-Field Specific Heat near T_N*

A preliminary analysis of our results has been given previously[25] but there are a number of important developments which warrant further discussion. Current theory indicates that specific heat should diverge at T_N according to

$$\frac{C}{R} = A_\pm \left| \frac{T - T_N}{T_N} \right|^{\alpha_\pm} + B_\pm , \tag{37}$$

where the suffix $\pm$ indicates $T \gtrless T_N$ and it is customary to write $\alpha_+ = \alpha$ and $\alpha_- = \alpha'$. This expression contains seven undetermined parameters and it is clearly not easy to fit them unambiguously, even

TABLE II. Single-ion parameters for DAG.

Parameter	Value	Method of determination
g_z	18.1 ± 0.2 [a]	Magnetization: $H \parallel [111]$ [b]
	18.0 [a]	c
	18.2 ± 0.2 [a]	d
	18.3 ± 0.3 [e]	Low-T, high-H specific heat [b]
	18.2 ± 0.2 [f]	Curie constant [b]
	18.0 ± 1.0	Neutron scattering [g]
	17.5 ± 0.9	Optical absorption [h]
	18.7	i
		j
	18.4 ± 0.5	
	18.3 ± 0.4	EPR of Dy^{3+} in YAG [k]
g_x, g_y	0.5 ± 0.2	Optical absorption [j]
	$\lvert g_x \pm g_y \rvert < 0.5$	Mössbauer effect [l]
	0.73 ± 0.15; 0.4 ± 0.2	EPR of Dy^{3+} in YAG [k]
λ_M (emu °K/mole)	10.45 ± 0.15	High-T susceptibility [b]
M_0 (111) (emu/cm^3)	666 ± 4	Low-T, high-H magnetization [b]
	670	c
χ_{VV} (emu/cm^3)	$(12.3 \pm 1.0) \times 10^{-4}$	Low-T, high-H magnetization [b,m]
a_0(Å)	12.04 ± 0.02 [n]	x-ray diffraction [o]
V_0 (cm^3)	43.8 ± 0.2 [n]	Calculated from x-ray structure [o]
$C_{hyp}T^2/R$ (°K)^2	$2.8 \times 10^{-3}(1 - 0.1/T)$	Calculated from EPR [p] and Mössbauer results (Ref. 1) [Eq. (8)]
	$(3.1 \pm 0.3) \times 10^{-3}$	Low-T zero-field specific heat [b]
Θ_D (°K)	500 ± 30	Estimated from specific heat of YAG and LuAG [q]
E_1/k_B (°K)	70.1 [r]	Optical absorption [h]
	70.3 [r]	i
	70.0 [r]	s
	70.2 [r]	Raman scattering [t]
	69 [r]	u

[a] More accurately this value corresponds to $\frac{1}{2}[(g_z^2 + 2g_x^2)^{1/2} + (g_z^2 + 2g_y^2)^{1/2}]$.

[b] This work.

[c] Reference 20, neglecting χ_{VV}.

[d] Reference 22, neglecting χ_{VV}.

[e] Assuming single value for $g_e = g_z/\sqrt{3}$.

[f] More accurately this value corresponds to $(g_x^2 + g_y^2 + g_z^2)^{1/2}$.

[g] Reference 21.

[h] Reference 10.

[i] Reference 8.

[j] Reference 11.

[k] Reference 6. The value of g_z is a somewhat more accurate redetermination of the published value 17.7 ± 0.7 [M. T. Hutchings (private communication)].

[l] Reference 23.

[m] Includes an estimated contribution of -0.02×10^{-4} emu/cm^3 from diamagnetism.

[n] Allows for variation between different samples and the effect of thermal contraction.

[o] References 15, 17, and 1.

[p] Reference 37.

[q] Reference 1. Note that Θ_D was defined in terms of only the Dy^{3+} ions. Including all atoms increases Θ_D by a factor 1.88 to (940 ± 60) °K.

[r] No error limits were quoted for any optical determinations of E_1 but the uncertainty is probably ~ 1 cm^{-1}. Within this range no difference was found between measurements made at 77 °K (Refs. 8, 10, 11, and 14) and those made at 1.5 °K (Ref. 79).

[s] Reference 12.

[t] Reference 79.

[u] Reference 14.

if good experimental data are available. However, in practice the problem is even more difficult, as there is always some rounding of the peak and the form of this cannot even be parametrized at the present time. Judging from the general similarity between the results found for four different DAG samples[50,59] it seems not entirely unlikely that at least some of the rounding may in fact be an intrinsic property in DAG and not only due to impurities or random strains, as is generally assumed.

However, if we neglect the rounding for the present and concentrate on the region which *seems* relatively unaffected (we can never be quite sure how large this is), we meet the difficulty that the asymptotic form of Eq. (37) should in fact be valid

TABLE III. Characteristic parameters determined from asymptotically exact theory.

Parameter	Value	Method of determination
Δ_0/k_B (°K)	7.60 ± 0.05	Low-T zero-field specific heat [a]
	7.2 ± 0.7	b
	7.54 ± 0.06	Low-T susceptibility [a]
	7.4	c
	7.62 ± 0.15	Optical absorption [d]
	7.58 ± 0.15	e
$-4U_0/R$ (°K)	7.68 ± 0.20	Integrated specific heat [a]
	7.6 ± 0.6	b
$H^c_{111}(0)$ (Oe)	3770 ± 40	Low-T magnetization [a]
	3780 ± 40	f
	3800 ± 60	Low-T latent heat [a]
	3900 ± 200	Optical absorption [e]
θ_1^{sphere} (°K)	0.04 ± 0.07	Low-T high-field specific heat [a]
	0.20 ± 0.15	High-T susceptibility [a]
	−0.13 ± 0.30	High-T high-field specific heat [a]
θ_2 (°K)^2	3.5 ± 0.4	High-T zero-field specific heat [a]
	3.7 ± 0.2	g
	3.1 ± 1.0	High-T high-H specific heat [a]
θ_3 (°K)^3	5.1 ± 3.0	High-T zero-field specific heat [a]
	6.0 ± 2.7	g

[a]This work.
[b]Reference 58.
[c]Reference 55.
[d]Reference 10.
[e]Reference 11.
[f]Reference 22.
[g]Reference 56.

only for values of $\epsilon = |(T - T_N)/T_N|$ less than some $\epsilon_c \sim 10^{-4}$, so that if there is any significant rounding, the true critical behavior will be completely concealed. It is quite pointless therefore to use an expression of the form of Eq. (37), even though an apparently satisfactory fit can be obtained.

Thus in our preliminary analysis we found an excellent fit to Eq. (37) with $\alpha' = 0$ (corresponding to a logarithmic divergence) for $10^{-4} < \epsilon < 5 \times 10^{-2}$, but this must now be regarded as an entirely empirical statement, and not related to theoretical predictions of the *asymptotic* form. *It is more than likely that a number of other critical-point specific-heat analyses reported in the literature are subject to the same limitations.*

In an attempt to extend the range of the theoretical predictions, Gaunt and Domb[60] constructed an interpolation formula linking the exact low-temperature expansion to the asymptotic form, and they were able to obtain a good fit to our data using only one adjustable constant T_N. In particular, they were able to show that the interpolation formula approximates closely to a logarithmic form in the range over which our data indicated such a variation, even though the asymptotic variation corresponds to $\alpha' = \frac{1}{8}$. However, any such fit can also not really be regarded as unique since it is necessarily based on a nearest-neighbor Ising model and thus neglects the complex nature of the actual interactions in DAG. It can be argued that these details are not important in the *critical* region, but they will surely affect the interpolation region to some extent. We can conclude from all this that it is going to be extremely difficult to fit the data below T_N with any expression based on simple theoretical approximations, and it would seem that only a detailed numerical calculation of the appropriate interpolation formula will ultimately prove to be completely satisfactory.

In the region above T_N the situation is slightly more hopeful since the asymptotic form should be valid over a considerably wider range ($\epsilon_c \sim 10^{-2}$), but as we shall see, there are still severe difficulties. The main problem, of course, is the fact that we still have to fit four parameters to an essentially smooth curve and this is hard to do unambiguously.

Due to the rounding we are first faced with the problem of determining T_N which will now not correspond to any infinite singularity. It is most tempting to choose the temperature of the experimental specific-heat maximum T_{max}, but Gaunt and Domb have argued that the effect of the rounding will in fact be such that the true T_N will be somewhat above T_{max}. Since there is no direct way of determining this difference we shall carry out three separate analyses taking $T_N = T_{max} + 1.3$ mK, $T_{max} + 0.3$ mK, and $T_{max} - 0.7$ mK in turn, and we shall compare the parameters resulting from the three different choices. We prefer this approach to a straightforward simultaneous fit of all four parameters since it demonstrates most clearly the importance of choosing the correct T_N, a point whose significance is frequently underestimated in analyses which do not display this effect explicitly.

Another factor whose importance is sometimes underestimated[61] is the constant B_+, which, though small compared with the singular term near T_N, may be quite comparable in the region over which the fit to Eq. (37) is made. If, as in the present case, one has closely spaced and accurate specific-heat data, one can eliminate the term B_+ by numerically differentiating the experimental results with respect to temperature and one can then plot $\ln|\partial/\partial T(C/R)|$ as a function of $\ln(T - T_N)/T_N$ for selected values of T_N to fit corresponding values of $1 + \alpha$ and A_+. Substituting these values back into the expression for C/R one can then find B_+. The results of this procedure, using the measurements on sample I of Paper I, are shown in Fig. 8,[62] and the corresponding parameters are summarized in Table IV, which includes also the values corresponding to a fourth choice for $T_N = T_{max} + 0.6$ mK. The variation of α, A_+, and B_+ with $T_N - T_{max}$ is shown graphically in Fig. 9.

It can be seen that changing T_N by only four parts in 10^4 affects the temperature range over which a fit is obtained and it also varies the corresponding constants α, A_+, and B_+ very significantly. If we assume that the deviations from a straight line in

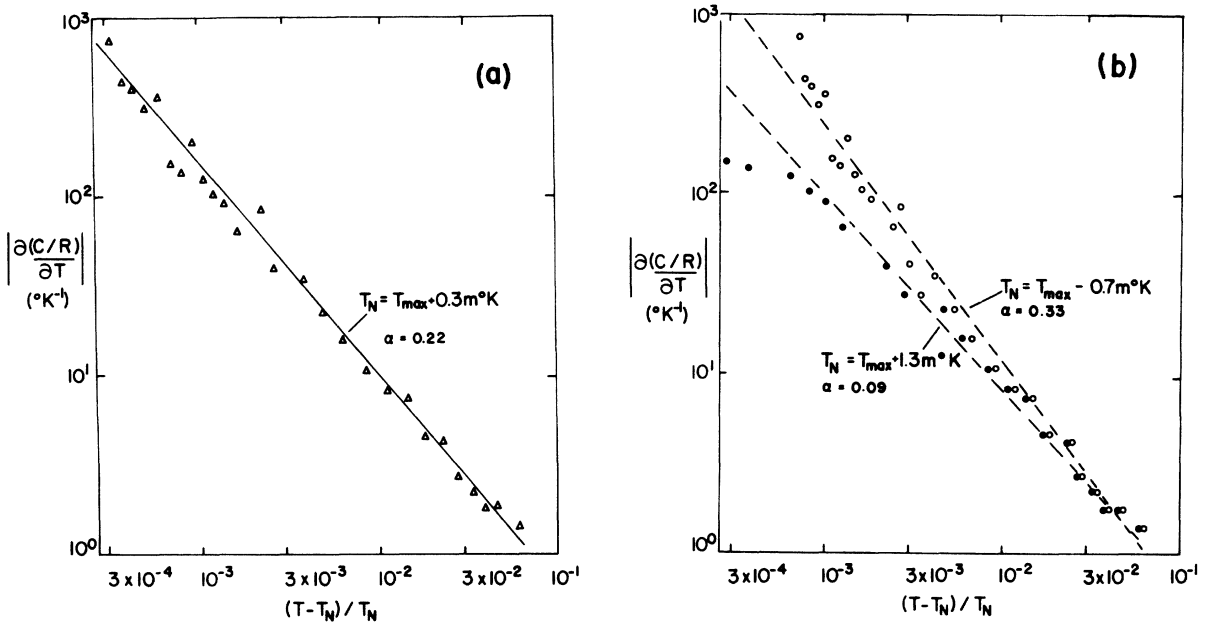

FIG. 8. Log-log plot of $|(\partial/\partial T)(C/R)|$ as a function of $(T-T_N)/T_N$, $(T>T_N)$, for three choices of T_N: (a) corresponds to the value $T_N = T_{max} + 0.0003$ °K; (b) shows the effect of changing T_N by ± 0.001 °K. The slopes of the fitted lines give corresponding values of $-(1+\alpha)$ and hence indicate that $0.1 \leq \alpha \leq 0.3$. Corresponding values for the parameters A_+ and B_+ are given in Table IV.

Fig. 8 at the lowest values of $(T-T_N)/T_N$ are genuine and not due to rounding effects, we might conclude that the middle choice of T_N gives the best fit, but the fit for the other values is almost as good, and it is really not possible to distinguish between them using only the available experimental data. It is almost certainly more significant that the upper choice for T_N leads to an α close to $\frac{1}{8}$, the value currently accepted as the correct exponent for three-dimensional Ising models, and it is interesting to note that this T_N would also be close to the value $T_{max} + 1.0$ mK proposed by Gaunt and Domb on the basis of their analysis of the data below T_N.[63] Moreover, we may note that for this value of T_N the other two constants are also close to the theoretical values calculated by Sykes *et al.*[64,65] for various cubic Ising models with nearest-neighbor interactions (see Table IV and Fig. 9). There is some indication[66] that the theoretical values for other lattices and interactions will not be too different, but a really critical comparison with theory is not possible at this time.

Part of the difficulty in analyzing the specific heat lies in the nature of singularity for $T > T_N$ which makes the fitted parameters so extremely sensitive to the particular choice of T_N, and in this connection it is of some interest to compare the variation of the parameters α, A_+, and B_+ with T_N with that found for the critical indices β, γ, and ν determined by neutron scattering.[67,68] In that case, a change in T_N of ± 1 mK resulted in changes of about ± 5, ± 15, and $\pm 12\%$, respectively, in the fitted values for β, γ, ν, which may be com-

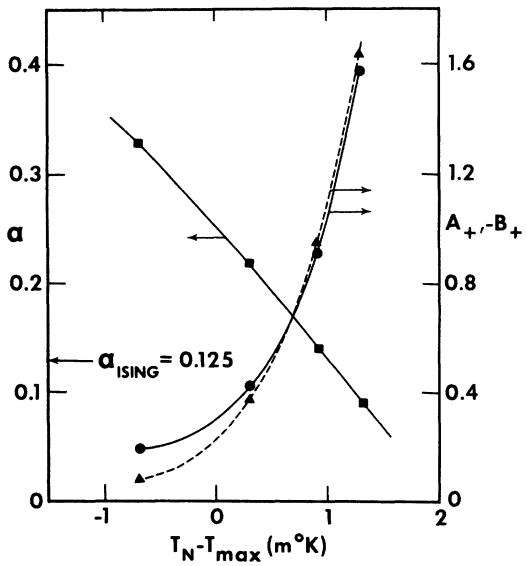

FIG. 9. Critical-point specific-heat parameters for $T > T_N$ as a function of $T_N - T_{max}$, with $T_{max} = 2.543_7$ °K. ■ shows variation of α (left scale); ●, ▲ show variation of A_+ and $-B_+$ (right scale). The theoretical value $\alpha = \frac{1}{8}$ would correspond to $T_N - T_{max} = 1.05$ mK and for this choice of T_N we find $A_+ = 1.10$ and $B_+ = -1.17$. These values may be compared with the results of the model calculations given in Table IV, which indicate $A_+ \approx 1.11$ and $B_+ \approx -1.24$.

TABLE IV. Critical-point specific-heat parameters for $T > T_N$, showing the effect of choosing different values for T_N, together with theoretical estimates for three cubic Ising models.[a]

$T_N - T_{max}$ (m °K)[b]	α	A_+	B_+
1.3	0.09	1.58	−1.64
0.6	0.14	0.91	−0.95
0.3	0.22	0.42	−0.37
−0.7	0.33	0.19	−0.08
theory sc[a]	0.125	1.136	−1.244
bcc[a]	0.125	1.106	−1.247
fcc[c]	0.125	1.088	−1.242

[a]Values calculated in Ref. 65 for the case of three cubic Ising models with nearest-neighbor interactions.

[b]All temperatures measured relative to $T_{max} = (2.543_7 \pm 0.010)$ °K for sample 1 of Ref. 1.

[c]See also Ref. 64.

pared with the change of more than ± 50% in α and ±(200 − 400)% in A_+ and B_+ for a similar variation in T_N here. It is clear therefore that the specific-heat parameters will always be intrinsically more uncertain, and we must conclude that it is simply not possible to set very close limits on the parameters in Eq. (37), even when as in the present case there are relatively good experimental results available ($\Delta T/T_N \sim 2 \times 10^{-5}$, $\Delta C/C < 0.04$). The only hope of improving this situation would seem to involve some additional information, experimental or theoretical.

The best solution, of course, would be to eliminate or substantially reduce the rounding but this may just not be possible and a useful alternative would be a more refined analysis taking account of the rounding, which would then also allow the use of experimental data closer to T_N. It would also make it possible to relate the results below T_N to those in the range above, and this should help to pin down the effective critical point. Another approach would be to construct a theoretical interpolation formula to allow a fit to the data over a greater range of $(T - T_N)/T_N$, as discussed for the region below T_N, but this is again complicated by the particular lattice structure of DAG and the fact that the interactions are not restricted to nearest neighbors. At this stage we can therefore only conclude that the specific heat above T_N is generally consistent with the variation predicted by the available approximate models, but a more detailed comparison is not possible.

It should perhaps be reemphasized that the difficulties which we have encountered here are not really peculiar to DAG and that similar analyses on other materials may also be subject to the same problems. Any purely empirical analysis of the specific heat in the critical region should therefore be examined very closely to ensure that the proposed fit is truly unique and not simply the result of some ephemeral prejudice.

2. *H-T Phase Boundary near T_N*

In the presence of fairly small applied magnetic fields (< 2.0 kOe) the observed specific-heat peaks remain quite sharp (see I), and while it was not possible to examine the shapes of the peaks in any detail, it was possible to estimate the variation of the ordering temperature with field quite accurately. For each pair of values of H_0 and T the corresponding internal field H_i was calculated using

$$H_i = H_0 - NM, \tag{38}$$

and a phase boundary of H_i^c vs T could thus be constructed. To analyze the shape of the curve, the results were fitted to an expression of the form

$$H_i^c = A_c[(T_N - T)/T_N]^n \tag{39}$$

and it was found that

$$n = 0.50 \pm 0.02,$$

$$A_c = 6.54 \pm 0.02 \text{ kOe},$$

$$T_N = (2.54 \pm 0.01)\ ^\circ\text{K}.$$

The value of $\frac{1}{2}$ for n is consistent with present theoretical models[69-72] which all agree that the phase boundary should be symmetrical in H and continuous through the point $(T_N, H = 0)$. To illustrate how well Eq. (39) fits the data, we have plotted in Fig. 10 $(H_i^c)^2$ vs T, and it can be seen that the fit is good to fields as high as 1.8 kOe, corresponding to a $\Delta T_N/T_N = 0.08$. At higher fields the experimental curve begins to increase more slowly and at $T = 0$ °K, H_i^c tends to about 3.8 kOe (see below), compared with the value $A_c = 6.54$ kOe.

3. *Magnetic Properties near Tricritical Point*

The experiments described in I showed that the nature of the phase change varies continuously along the phase boundary, becoming sharper as H increases, until it suddenly becomes first order at a point $T_t = 1.66$ °K, $H_i^t = 3.25$ kOe, and $M_t = 250$ emu/cm^3. The approach of the first-order transition is signaled already above T_t by a marked increase in the maximum slopes of the $M - H_i$ isotherms, which appear to be definitely finite (within the experimental resolution) but tend to infinity as $T \to T_t$. There is no detailed theory of any kind for this behavior but we can guess that the divergence may be described by a law of the form

$$\left(\frac{\partial M}{\partial H_i}\right)_{max} \equiv \chi_c = P\left(\frac{T - T_t}{T_t}\right)^r, \tag{40}$$

where P is a constant. As explained in I it was unfortunately not possible to obtain experimental values of χ_c very near T_t, but we can obtain approxi-

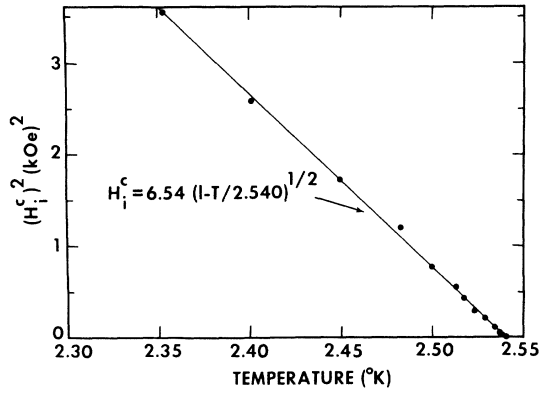

FIG. 10. Phase boundary for DAG near T_N for fields along [111]. All fields have been converted to the sample-shape-independent internal field H_i using Eq. (38). The solid line through the experimental points represents the relation $H_i^c = A_{111}^c[(T_N - T)/T_N]^n$ with $T_N = (2.54 \pm 0.01)$ °K, $A_{111}^c = 6.54 \pm 0.02$ kOe, and $n = 0.50 \pm 0.02$.

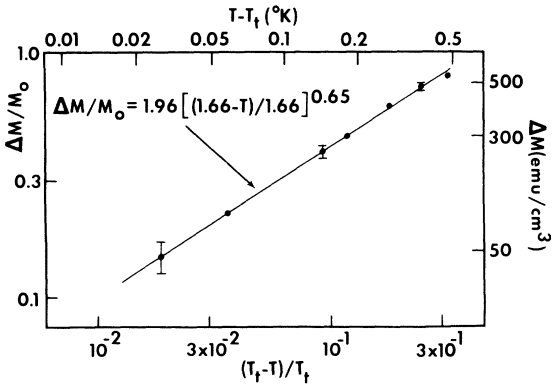

FIG. 12. Temperature dependence of the magnetization discontinuity across the first-order phase transition in DAG for fields along [111] near the tricritical point. The log-log plot shows that the variation of ΔM is consistent with a law of the form $\Delta M/M_0 = R[(T_t - T)/T_t]^\rho$ with $R = 1.96 \pm 0.09$, $\rho = 0.65 \pm 0.05$, and $T_t = (1.66 \pm 0.01)$ °K as determined from the divergence of χ_c.

mate values for the parameters in Eq. (40) from data at somewhat higher temperatures. Figure 11 shows a plot of $\ln\chi_c$ as a function of $\ln(T - T_t)/T_t$ from which we find

$$\pi = -1.3 \pm 0.1,$$

$$P = 0.1 \pm 0.03 \text{ emu/cm}^3,$$

$$T_t = (1.66 \pm 0.01)\ ^\circ\text{K}.$$

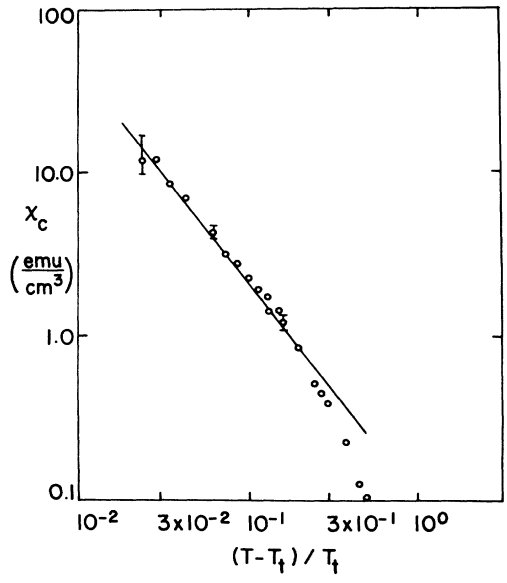

FIG. 11. Temperature dependence of the critical susceptibility along the [111] phase boundary of DAG defined by $\chi_c = (\partial M/\partial H_i)_{max}$. The log-log plot shows that the divergence of χ_c as T approaches the tricritical point is consistent with a law of the form $\chi_c = P[(T - T_t)/T_t]^\pi$ with $P = 0.10 \pm 0.03$ emu/cm^3, $T_t = (1.66 \pm 0.01)$ °K, and $\pi = -1.3 \pm 0.1$.

Equation (40) may also be rewritten in a possibly more convenient dimensionless form

$$\chi_c T/\lambda = P'[(T - T_t)/T_t]^{\pi'}, \tag{40a}$$

where λ is the Curie constant. Using this form we find

$$P' = 1.05 \pm 0.25,$$

$$\pi' = -1.2 \pm 0.1.$$

Below T_t the magnetization shows a typical first-order discontinuity, $\Delta M = M^+ - M^-$, which tends to zero as T increases towards T_t, and we can attempt to fit another asymptotic law to this variation. We shall assume for simplicity that

$$(M^+ - M^-)/M_0 = R[(T_t - T)/T_t]^\rho, \tag{41}$$

though it may in fact be more appropriate to fit separate laws of this form to M^+ and M^- individually.[73] As explained in I, it is experimentally very difficult to make any really accurate statements about M^+ or M^- so that we must content ourselves with the simpler form of Eq. (41). Choosing T_t to have the same value as indicated by the analysis of χ_c, we obtain the plot of $\ln(\Delta M)/M_0$ as a function of $\ln(T_t - T)/T_t$ shown in Fig. 12. The fit to a straight line is quite good but we must allow for possible uncertainties in both T_t and ΔM and we finally conclude that

$$\rho = 0.65 \pm 0.05,$$

$$R = 1.96 \pm 0.09.$$

The only quantitative theory for this type of behavior is given by the mean field approximation,[69,74,75] and this predicts $\rho = 1$ in apparent contradiction to the present results. This is of course

not very surprising, but it is clear that more realistic theories will have to be quite subtle to reproduce the type of behavior which is observed. There have recently been some new theoretical conjectures by Griffiths concerning the nature of tricritical points[5] and it will be interesting to see if these will explain our results. In this connection it must be cautioned that the present experiments do not really cover the region in the immediate vicinity of the tricritical point, so that the true asymptotic behavior could well be different from that inferred here if the critical region were in fact quite small. In any case it would seem clear that further theoretical and experimental studies of the region of the tricritical point are called for.

4. *Extrapolation of Critical Field to* $T = 0\,^{\circ}\mathrm{K}$

Even in the absence of a general theory of the first-order phase transition, there is some interest in extrapolating the phase boundary to $T = 0\,^{\circ}\mathrm{K}$ since in this limit a very simple analysis is again possible.

One way of estimating $H^c(0)$ is to use the fact that M^+ and M^- tend to M_0 and 0, respectively,[76] as $T \to 0\,^{\circ}\mathrm{K}$, so that plots of $H_i^c(T)$ against $M^+(T)$ and $M^-(T)$ should extrapolate to a common value of $H^c(0)$ as $M^+ \to M_0$ and $M^- \to 0$.

This extrapolation was carried out in the manner prescribed by molecular field theory.[75] From the asymptotic approach of H^c, M^+, and M^- to their $T = 0\,^{\circ}\mathrm{K}$ values we find the following relationships:

$$\zeta^- = M^- T = \frac{2 g_e \mu_B M_0}{k_B} \left[H_i^c(T) - H_i^c(0) \right],$$
$$\zeta^+ = (M_0 - M^+) T = \frac{4 g_e \mu_B M_0}{k_B} \left[H_i^c(T) - H_i^c(0) \right]. \tag{42}$$

Plots of ζ^- and ζ^+ vs H_i^c should thus be straight lines, having slopes proportional to g_e and intercepts equal to $H_i^c(0)$. Using the measurements given in I, corrected for second-order effects by Eq. (5), we find the results shown in Fig. 13, and these yield the values

$$H_i^c(0) = 3770 \pm 40\,\mathrm{Oe}, \quad g_e = 10.1 \pm 1.0.$$

Although the errors in the slopes are larger than we would have liked, the length of the extrapolation is quite short and the uncertainty in $H_i^c(0)$ is quite small. A linear extrapolation of $M^{\pm}$ vs H_i^c yields a critical field about 5 Oe greater than the above value, but there is no theoretical justification for preferring this latter method.

A value of $H_i^c(0)$ can also be obtained by extrapolating the results of the isothermal field sweeps described in I. The advantage of using these measurements in the present case is that they extend down to much lower temperatures than the magnetic moment data, so that a much smaller extrapolation is needed. On the other hand, these measurements only yield values for the *external* fields $H_0^+(T)$ and $H_0^-(T)$, and the correction to $H_i^c(T)$ would again require knowledge of $M(T)$ which is not available in the interesting range. However, if we are interested only in $T = 0\,^{\circ}\mathrm{K}$, we can apply the demagnetizing correction without any additional measurements, since we know that the correction will be approximately zero for $H_0^-(0)$ and NM_0 for $H_0^+(0)$. As before there will be small additional corrections due to the temperature-independent susceptibility but these can also be calculated. Corresponding to the values of $m_0^{\pm}$ given in Ref. 76, there will be additional demagnetizing fields $Nm_0^- = 25\,\mathrm{Oe}$ and $Nm_0^+ = 56\,\mathrm{Oe}$ which must be applied to $H_0^-(0)$ and $H_0^+(0)$, respectively. Figure 14 shows graphs of $h^- = H_0^-(T) - Nm_0^-$ and $h^+ = H_0^+(T) - N(M_0 + m_0^+)$ as functions of T, and it can be seen that both extrapolate to approximately the same value of $T = 0\,^{\circ}\mathrm{K}$, with dH^c/dT tending to zero at $T \to 0\,^{\circ}\mathrm{K}$. The small difference between the two limits is almost certainly due to an error in the demagnetizing correction to $H_0^+(0)$, since this amounts to more than 3.5 kOe, so that the discrepancy corresponds to an error of only about 2%. We therefore attach a much larger weight to the extrapolated value for H_0^- and we conclude that this method gives

$$H_i^c(0) = 3800 \pm 60\,\mathrm{Oe},$$

in excellent agreement with the value obtained previously.

Both values are also in good agreement with a determination by Bidaux *et al.*[22] who made magne-

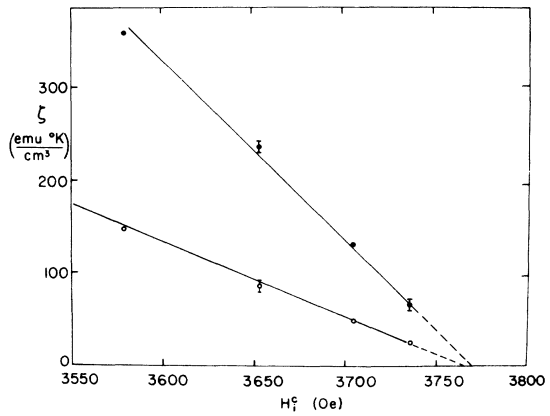

FIG. 13. Determination of critical field at absolute zero, $H_i^c(0)$, from low-temperature magnetization measurements with H along [111]. ooo = experimental values of $\zeta^- = M^- T$ and ●●● = experimental values of $\zeta^+ = (M_0 - M^+)T$, where $M^{\pm}$ denote the end points of the first-order discontinuity [corrected for small second-order effects according to Eq. (5)], and $M_0 = 666$ emu/cm^3 is the saturation magnetization. The intercepts on the abscissa give $H_c^i(0) = 3770 \pm 40$ Oe.

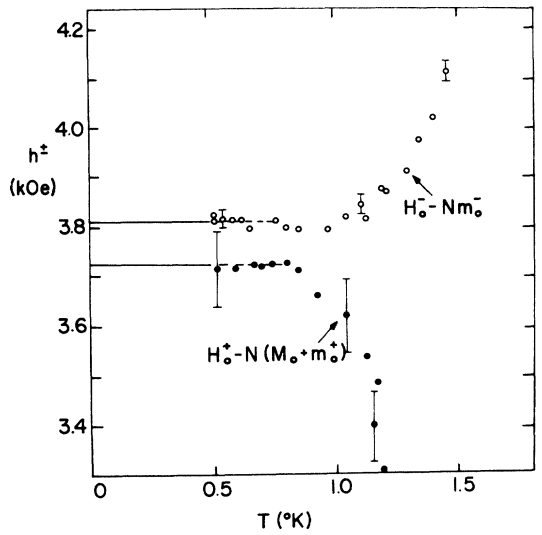

FIG. 14. Determination of critical field of DAG at absolute zero, $H_i^c(0)$, from low-temperature latent-heat measurements with H along [111]. ○○○ = experimental values of $h^- = H_0^- - Nm_0^-$ and ●●● = experimental values of $h^+ = H_0^+ - N(M_0 + m_0^+)$, where $H_0^\pm$ denote the end points of the first-order transition as measured on a sample with demagnetizing factor N, M_0 is the saturation magnetization (666 emu/cm^3), and $m_0^\pm$ are small second-order corrections as given in Ref. 76. Ideally, the two curves should extrapolate to the same value at $T = 0$ °K giving $H_i^c(0)$. The error bars indicate a 2% uncertainty in the demagnetizing corrections plus the estimated errors in determining $H_0^\pm$. Combining the weighted results gives $H_i^c(0) = 3800 \pm 60$ Oe.

tization measurements at very low temperatures (0.37 °K), and they are also in agreement with values estimated from optical data,[11] but these were obtained at higher temperatures and are not quite so accurate.

All these results confirm an assumption which we have made implicitly throughout but which is not necessarily valid under all circumstances, namely that there are really only two phases, the antiferromagnetic and the paramagnetic. Since the interactions are not *identically* Ising-like it would appear possible that there might be another phase, corresponding to the normal spin-flop phase in more isotropic antiferromagnetics, and this would appear at the upper end of the first-order transition, before the final transition to the paramagnetic state. Experimentally such an extra phase would manifest itself as a flattening of the upper corner of the magnetization curve, and this in turn would make $\Delta M < M_0$ at $T = 0$ °K. The agreement between the different extrapolations of the upper and lower ends of the observed phase transition indicates that $\Delta M(T = 0)$ is in fact very close to M_0 and this shows that the spin-flop phase if present would be restricted to a very narrow range of field. In fact, there is no indication of any kind that such a phase is really present in DAG and it seems safe to assume that the interactions are such as to make it energetically unfavorable. The microscopic conditions for this have been discussed by Gorter and van Peski-Tinbergen,[74] and will be reviewed in Paper IV.

5. *Thermodynamic Functions at Critical Points*

It may be of interest for later microscopic calculations to list some of the values of the two principal thermodynamic functions, the internal energy and the entropy at a number of critical points on the phase diagram. Taking the zero of U at $T = \infty$ [44] and that of S at $T = 0$ °K, we find from the curves given in I the values listed in Table V. These results are generally in good agreement with earlier somewhat less accurate measurements made on a polycrystalline sample of DAG.[58]

Most of the thermodynamic parameters will become significant only in the context of detailed statistical calculations, but at least one of them $[U(0, 0)]$ can be interpreted directly in terms of a simple picture of the ground state as discussed previously. We shall pursue this analysis in Paper IV.

6. *Summary of Critical Parameters*

The parameters determined in the previous sections are summarized in Tables IV–VI. In contrast to the single-ion and collective parameters, none of these have any immediate microscopic interpretation in terms of our simple model Hamiltonian, since they describe complex many-body effects which can only be discussed using detailed calculations of the statistical mechanics. Unfortunately none of the calculations which have been made so far are directly applicable, since DAG has an unusual cubic-lattice structure and interactions which extend beyond nearest neighbors,[77] but we might hope that the wealth of data now available will stimulate such studies. One may also hope for further developments in the general theory of tricritical points which may make it possible to interpret some of the new parameters which have been determined here, but at this stage they can only be viewed as providing an empirical description of an interesting and com-

TABLE V. Internal energy and entropy at critical points after Ref. 1.

T, H_i	U/R	S/R
∞, 0	0	0.702 ± 0.010 (0.693 calc)
T_N, 0	-0.87 ± 0.03	0.518 ± 0.005
T_t, H_i^t	-0.92 ± 0.05	0.330 ± 0.010
0, 0	-1.92 ± 0.05	0

TABLE VI. Critical parameters describing phase boundary.

Region	Parameter	Value	Method of determination
Zero-field critical point			
	T_N (°K)	2.55 ± 0.01 [a]	Susceptibility [b]
		2.49 ± 0.01 [a]	Specific heat [c]
		2.54 ± 0.02 [a]	Neutron diffraction [d]
		$2.51_7 \pm 0.01$ [a]	Neutron scattering [e]
		$2.54_5 \pm 0.01$ [a]	Specific heat [f]
	α	0.2 ± 0.1	Specific heat $T > T_N$ [f]
	α'	g	Specific heat $T < T_N$ [f]
	β	0.26 ± 0.02	Neutron scattering $T < T_N$ [h]
	γ	1.16 ± 0.04	Neutron scattering $T < T_N$ [e]
	ν	0.61 ± 0.02	e
	η	0.12 ± 0.10	e
Phase boundary near T_N			
	A^c_{111} (kOe)	6.54 ± 0.02	Magnetization and specific heat in low fields [f]
	n	0.50 ± 0.02	
Tricritical point			
	T_t(°K)	1.66 ± 0.01	Magnetization and specific heat [f]
	R	1.96 ± 0.09	Magnetization $T < T_t$ [f]
	ρ	0.65 ± 0.05	f
	P (emu/cm^3)	0.10 ± 0.03	Differential susceptibility $T > T_t$ [f]
	π	-1.3 ± 0.1	f

[a]The error limits for T_N represent estimates of the calibration uncertainties which are generally much larger than the errors in locating T_N on a relative temperature scale. The apparent discrepancies between the different T_N values are almost certainly due to genuine differences between the samples studied, as discussed in the text.

[b]Reference 6.

[c]Reference 58.

[d]Reference 21.

[e]Reference 68.

[f]This work.

[g]Data for $T < T_N$ could be fitted by $C/R = A_- \ln(T_N - T)/T_N + B_-$ with $A_- = -0.485 \pm 0.015$ and $B_- = 0.45 \pm 0.06$ for $3 \times 10^{-4} < (T_N - T)/T_N < 3 \times 10^{-2}$, but this is outside the true critical region, as discussed in Ref. 60.

[h]Reference 67.

plex phenomenon.

It is perhaps worth commenting at this point that there are also still some experimental problems in the detailed understanding of DAG related to the observed variation in the value of T_N and the "rounding" of high-resolution data in the immediate vicinity of T_N. Thus one can find in the literature different estimates for T_N ranging from 2.49 to 2.55 °K, [1,6,21,58,68] a surprisingly large variation in view of the relative ease of measuring temperatures in this region. Some of these differences may in fact be due to uncertainties in absolute temperature calibrations, for which errors were generally not quoted, but to some extent the variation is real and must be ascribed to actual differences between the samples used. In particular, the low value of 2.49 °K was only found for a flame-fusion-grown polycrystalline sample which also contained a small impurity of the perovskite $DyAlO_3$, [58] but even single crystals grown by the same method showed T_N's varying over 0.023 °K. [1] At this stage we can therefore only conclude that "good quality" DAG has a T_N which falls in the range (2.53 ± 0.02)°K, with any particular sample having a value which can be determined to within ± 0.001 °K, plus any uncertainty on the absolute-temperature calibration.

Effects of this kind are of course important only in quite detailed studies involving the correlation of several different sets of experimental data, but it is the possibility of just such comparisons that makes DAG such an attractive material for thorough analysis. For the moment, by far the biggest problems lie with the theory but one may hope that the experimental situation will also be clarified in the future.

V. SUMMARY

In this paper we have analyzed the available magnetothermodynamic measurements on DAG using a semimicroscopic approach. Without considering specific details of the spin-spin interactions, it has been possible to show that DAG in a magnetic field

along a ⟨111⟩ axis closely resembles a two-sublattice Ising antiferromagnet and we have considered in some detail the various factors which might cause small deviations from the ideal Ising approximations. It is shown that these are indeed all very small in the case of DAG, but this is not necessarily so in other systems which might sometimes *appear* to be Ising-like.

Using the Ising-model approximation we have then derived a number of asymptotically exact general expressions relating the thermal and magnetic properties to certain combinations of terms in the microscopic spin Hamiltonian, and we have used these to determine a number of characteristic parameters describing DAG. These parameters are of three kinds.

The first are *single-ion* parameters which describe the properties of the individual Dy^{3+} ions in their interactions with applied fields, their nuclear moments, and optical radiation. These parameters are summarized in Table II, which also includes a number of other useful constants describing the general properties of DAG.

The second kind are *collective* parameters, which involve the effective spin-spin interactions in various combinations to describe macroscopic properties in the regions where asymptotically exact theoretical expressions are valid. The results of this type of analysis are summarized in Table III. Clearly, all these parameters are not independent, but we shall defer any correlation until Paper IV of the present series,[4] where we shall reduce the parameters to a single set consistent within the limits of experimental uncertainty and extract a corresponding set of *microscopic* parameters. A preliminary analysis of this sort has already demonstrated that a generally satisfactory solution can be obtained[22,25] (see also Refs. 50 and 55), but we shall show that some further refinement is, in fact, possible.

In addition to these two kinds of parameters, we have also been able to extract a third set which characterizes the critical properties and which can only be related to the microscopic Hamiltonian using more detailed statistical calculations. These critical parameters are summarized in Tables IV and VI, and some of the corresponding thermodynamic functions are given in Table V. These parameters will be discussed in Paper V of the present series.[78]

However, even without detailed microscopic analyses it is already clear at this stage that while DAG corresponds very closely to a simple Ising antiferromagnet in some respects, it differs in one very important property, in that its interactions are not exclusively short ranged. In this respect it is similar to *all* real magnetic systems and it would seem well worth while at this stage to make renewed attempts to extend the theory of the Ising model to include more realistic interactions. If such calculations could be made, DAG would serve as an excellent test of the theoretical predictions.

ACKNOWLEDGMENTS

We would like to thank M. Blume, C. Domb, R. Faulhaber, M. E. Fisher, I. Nowik, J. G. Park, and H. Wagner for a number of helpful and stimulating discussions, and A. T. Skjeltorp and E. A. Wolf for checking several of the theoretical expressions and for critical reading of the manuscript. One of us (W. P. W) would also like to thank the Physics Department of the Brookhaven National Laboratory for their gracious hospitality during the preparation of the final draft of this paper.

---

*Work supported in part by the U. S. Atomic Energy Commission.

†Present address: Philips Forschungslaboratorium, 2000 Hamburg 54, Germany.

‡Present address: Department of Physics, University of Georgia, Athens, Ga. 30601.

§Present address: United Kingdom Atomic Energy Authority, Culham Laboratory, Culham, Berks., England.

[1]D. P. Landau, B. E. Keen, B. Schneider, and W. P. Wolf, Phys. Rev. B 3, 2310 (1971), Paper I in the present series.

[2]See, for example, F. Keffer, in *Handbuch der Physik*, edited by H. P. J. Wijn (Springer, Berlin, 1966), Vol. 18, Part 2, p. 1.

[3]B. E. Keen, D. P. Landau, and W. P. Wolf (unpublished), Paper III in the present series.

[4]B. Schneider, D. P. Landau, B. E. Keen, and W. P. Wolf (unpublished), Paper IV in the present series.

[5]R. B. Griffiths, Phys. Rev. Letters 24, 715 (1970).

[6]M. Ball, M. T. Hutchings, M. J. M. Leask, and W. P. Wolf, in *Proceedings of the Eighth International Congress on Low Temperature Physics* (Butterworths, London, 1963), p. 248.

[7]R. C. Milward, Phys. Letters 25A, 19 (1967).

[8]K. Aoyagi, K. Tsushima, and M. Uesugi, J. Phys. Soc. Japan 27, 49 (1969).

[9]S. Washimiya, J. Phys. Soc. Japan 27, 49 (1969).

[10]K. A. Gehring, M. J. M. Leask, and J. H. M. Thronley, J. Phys. C 2, 484 (1969).

[11]R. Faulhaber and S. Hüfner, Z. Physik 228, 235 (1969).

[12]P. Grünberg, S. Hüfner, E. Orlich, and J. Schmitt, Phys. Rev. 184, 285 (1969).

[13]J. Blanc, D. Brochier, and A. Ribeyron, Phys. Letters 33A, 201 (1970).

[14]R. L. Wadsack, Joan L. Lewis, B. E. Argyle, and R. K. Chang, Phys. Rev. B 3, 4342 (1971).

[15]F. Bertaut and F. Forrat, Compt. Rend. 244, 96 (1957).

[16]S. Geller and M. A. Gilleo, J. Phys. Chem. Solids 3, 30 (1957).

[17]K. L. Keester and G. G. Johnson, Jr., J. Appl.

Cryst. 4, 178 (1971).

[18]See, for example, Ref. 6.

[19]W. P. Wolf, Proc. Phys. Soc. (London) 74, 65

[20]M. Ball, W. P. Wolf, and A. F. G. Wyatt, Phys. Letters 10, 7 (1964).

[21]A. Herpin and P. Mériel, Compt. Rend. 259, 2416 (1964).

[22]R. Bidaux, P. Carrara, and B. Vivet, J. Phys. 29, 357 (1968).

[23]I. Nowik and H. H. Wickman, Phys. Rev. 140, A869 (1965).

[24]We wish to thank Dr. I. Nowik for supplying a copy of the computer program which was used to calculate the Dy^{161} Mössbauer spectra (Ref. 23). A very careful analysis of two groups of transition lines which are particularly sensitive to the hyperfine constants A_x, A_y was used to determine the upper limits on $|A_x+A_y|$ and $|A_x-A_y|$. As is pointed out in Sec. II C 4, A and g are proportional, and one can therefore place limits on $|g_x+g_y|$ and $|g_x-g_y|$.

[25]B. Schneider, D. P. Landau, B. E. Keen, and W. P. Wolf, Phys. Letters 23, 210 (1966).

[26]J. L. Lewis, thesis (Yale University, 1971) (unpublished).

[27]R. J. Birgeneau, M. T. Hutchings, and R. N. Rogers, Phys. Rev. Letters 16, 584 (1965).

[28]J. M. Baker, R. J. Birgeneau, M. T. Hutchings, and J. D. Riley, Phys. Rev. Letters 21, 620 (1968).

[29]We use the convention that μ_B, the Bohr magneton, is a positive quantity.

[30]J. H. Van Vleck, *The Theory of Electric and Magnetic Susceptibilities* (Oxford U.P., London, 1932).

[31]W. H. Brumage, C. C. Lin, and J. H. Van Vleck, Phys. Rev. 132, 608 (1963).

[32]B. Schneider (unpublished).

[33]M. E. Fisher, Phys. Rev. 176, 257 (1968).

[34]H. Wagner, Phys. Rev. Letters 25, 31 (1970).

[35]C. Domb and J. A. Wyles, J. Phys. C 2, 2435 (1969).

[36]J. I. Philip, R. Gonano, and E. D. Adams, J. Appl. Phys. 40, 1275 (1969).

[37]J. G. Park, Proc. Roy. Soc. (London) A254, 118 (1958).

[38]R. J. Elliot and K. W. H. Stevens have shown (Ref. 39) that as long as the crystal-field states are spanned by a single J multiplet A_α and g_α are proportional. The ground-state wave function for Dy^{3+} in DAG is almost completely $J=\pm\frac{15}{2}$ (see Ref. 26) and therefore we would expect this proportionality to hold.

[39]R. J. Elliot and K. W. H. Stevens, Proc. Roy. Soc. (London) A218, 553 (1953).

[40]D. C. Mattis and W. P. Wolf, Phys. Rev. Letters 16, 899 (1966).

[41]B. Bleaney, Phil. Mag. 42, 441 (1951).

[42]One possible source of additional specific heat at low temperatures would be a magnetic impurity subject to an internal field from the aligned Dy^{3+} spins, and an order of magnitude estimate shows that as little as 0.5% of impurity (or Dy^{3+} ions on wrong crystal sites) could account for the observed excess specific heat. However, the effect is probably more complicated, as the observed excess does not show a significant field dependence whereas that due to a simple impurity would. More detailed measurements below 1 °K are needed to resolve this.

[43]We are indebted to M. E. Fisher and D. C. Mattis for helpful discussions of this question.

[44]In taking the asymptotic limits "to infinity" it is to be understood that $g_e\mu_B H_0$ and $k_B T$ are still small compared with E_1, the energy of the first excited electronic state, so that the effective-spin approximation can be used throughout.

[45]J. H. Van Vleck, J. Chem. Phys. 5, 320 (1937).

[46]W. Opechowski, Physica 4, 181 (1937).

[47]J. M. Daniels, Proc. Phys. Soc. (London) 66, 673 (1953).

[48]As discussed in I, there is some uncertainty in the lattice parameter appropriate to a particular DAG sample due to variations in stoichiometry, but the effect is very small (~0.1%). There is also an additional uncertainty due to thermal contraction, since the only x-ray studies so far (Refs. 15–17) were made at room temperature. Our best estimate for the effective lattice parameter is thus $a_0=12.04\pm0.02$ Å which corresponds to a gram-atomic volume $V_0=43.8\pm0.2$ cm^3.

[49]A more detailed discussion as well as an extension to a more complex form for the interaction Hamiltonian may be found in Ref. 50. It should be noted however that there are some numerical errors in Ref. 50 which have been corrected here (see also Ref. 51).

[50]D. P. Landau, thesis (Yale University, 1967) (unpublished).

[51]A. T. Skjeltorp, thesis (Yale University, 1971) (unpublished).

[52]A. R. Wakefield, Proc. Cambridge Phil. Soc. 47, 419 (1951).

[53]As in any extrapolation procedure, one must beware of overestimating the accuracy of such a trick. In the present case it seems justified since the contributions to Eq. (23) arising from multiple excitations will themselves be functions of $\exp(-\Delta_0/k_BT)$ which go to zero smoothly with C/R. We are indebted to J. C. Bonner for a discussion of this problem.

[54]The method could even be extended for studying the anisotropy of g, but in a system such as the garnet with several ions per unit cell this would in general entail separating several superimposed exponential specific-heat tails and this may not always be possible.

[55]A. F. G. Wyatt, thesis (Oxford University, 1963) (unpublished).

[56]A. T. Skjeltorp and W. P. Wolf, AIP Conf. Proc. (USA) 5, 695 (1971).

[57]See, for example, W. P. Wolf and J. F. Heinz, J. Appl. Phys. 36, 1127 (1965).

[58]M. Ball, M. J. M. Leask, W. P. Wolf, and A. F. G. Wyatt, J. Appl. Phys. 34, 1104 (1963).

[59]B. E. Keen, D. P. Landau, and W. P. Wolf, J. Appl. Phys. 38, 967 (1967).

[60]D. S. Gaunt and C. Domb, J. Phys. C 1, 1038 (1968).

[61]See, for example, Ref. 59.

[62]The results for the other samples have not been reanalyzed in such detail but judging from the general similarity of the experimental curves it seems quite likely that the critical parameters will be quite similar, except for the variation in T_{max} already discussed in I.

[63]*Footnote added in proof.* A similar conclusion has also been reached by D. L. Hunter, thesis (London University, 1967) (unpublished). We are grateful to Professor Domb for informing us about this work.

[64]M. F. Sykes, J. L. Martin, and D. L. Hunter, Proc. Phys. Soc. (London) 91, 671 (1967).

[65]M. F. Sykes, D. L. Hunter, D. S. McKenzie, and B. R. Heap (unpublished). We are grateful to Professor C. Domb for informing us about this work prior to publi-

cation.
[66]C. Domb (private communication).
[67]J. C. Norvell, W. P. Wolf, L. M. Corliss, J. M. Hastings, and R. Nathans, Phys. Rev. 186, 557 (1969).
[68]J. C. Norvell, W. P. Wolf, L. M. Corliss, J. M. Hastings, and R. Nathans, Phys. Rev. 186, 567 (1969).
[69]K. Motizuki, J. Phys. Soc. Japan 14, 759 (1959).
[70]M. E. Fisher, Proc. Roy. Soc. (London) A254, 66 (1960).
[71]D. M. Burley, Physica 27, 768 (1961).
[72]A. Bienenstock, J. Appl. Phys. 37, 1459 (1966).
[73]We are indebted to H. Wagner for a discussion of this point.
[74]C. J. Gorter and T. van Peski-Tinbergen, Physica 22, 273 (1956).
[75]R. Bidaux, P. Carrara, and B. Vivet, J. Phys. Chem. Solids 28, 2453 (1967).
[76]After allowing for the small contributions arising from the temperature-independent susceptibility $m = \chi_{VV}(H_0 + aM)$ [Eq. (5)]. For $M^-(0)$ this amounts to about $m_0^- = 4.7$ emu/cm^3, while for $M^+(0)$ the contribution is about $m_0^+ = 10.4$ emu/cm^3.
[77]A good summary of the available information on the range dependence of the interactions and their relation to the structure of DAG may be found in Ref. 67.
[78]D. P. Landau, B. Schneider, and R. Faulhaber (unpublished).
[79]B. E. Argyle, J. L. Lewis, R. L. Wadsack and R. K. Chang, Phys. Rev. B 4, 3035 (1971).

PHYSICAL REVIEW B VOLUME 5, NUMBER 11 1 JUNE 1972

Theory of Verwey and Charge-Density-Wave-State Ordering in Magnetite

J. B. Sokoloff*†
Physics Department, Northeastern University, Boston, Massachusetts 02115
and
Physics Department, Bar-Ilan University, Ramat-Gan, Israel

The Cullen-Callen Hartree-approximation band model of magnetite is solved self-consistently, and it is found that if one starts with the three-order-parameter state of Cullen and Callen, the solution iterates self-consistently to the Verwey ordered state. A charge-density-wave-state ordering is proposed to explain recent neutron- and electron-diffraction, magnetic-resonance, and Mössbauer-effect experiments on magnetite, which suggest a larger unit cell than occurs in the Verwey ordering. It is argued that the Verwey ordering could very easily be unstable to the formation of such a state. A discussion is also given of small polarons in a degenerate electron system and applied to magnetite.

I. INTRODUCTION

Recently, Cullen and Callen have proposed that the low-temperature insulating phase of magnetite (i.e., below 120 °K) could be described by a Hartree-approximation band model in which the Hartree self-consistent field does not have the full symmetry of the lattice.[1] Within such a model, it is possible to have a Verwey-type ordering[2]—that is, an octahedral-site charge density per site which alternates between two values on adjacent planes of octahedral sites along one of the crystallographic axes called the c axis.[3,4] (See Fig. 1 in Ref. 4.) The octahedral-site ions, however, need not be pure Fe^{+3} or Fe^{+2} as originally suggested by Verwey.[2] Recent neutron-diffraction,[5] electron-microscopy,[6] Mössbauer-effect,[7,8] and magnetic-resonance[8] experiments have shown that the ordering is apparently more complicated than the simple Verwey ordering. In this paper, the Cullen and Callen model is reinvestigated. A self-consistent calculation shows that the three-parameter ordering suggested in Ref. 1 does not lead to a self-consistent solution of the Hartree-approximation equations. Rather, it is found that if we start with the three-parameter ordering, successive interactions in the self-consistency scheme take us towards the Verwey ordering. It is proposed that experimentally observed deviations from the Verwey state can be explained as being due to an instability of the Verwey state to the formation of an excitonic insulating state. It is further shown that if the Verwey order parameter is chosen small enough for the insulating gap to just disappear, a gap is not produced by also introducing the two additional order parameters suggested by Cullen and Callen. This fact together with the self-consistency calculation, which is done for larger values of the Verwey order parameter, cast doubt on the existence of the three-parameter ordering, although it is admittedly possible that for some particular values of the three order parameters suggested by Cullen and Callen, a self-consistent solution might be possible. Although no gap is introduced at the point $\vec{k} = (0, 0, \pi/a)$, it is still possible for a gap to appear at other points in the zone. Thus, the results are not conclusive.

II. SELF-CONSISTENCY OF THE CULLEN-CALLEN MODEL

Following Cullen and Callen, we assume a clos-